CHAPTER 3

MATERIALS AND METHODOLOGY

3.1 Preface

This chapter presents the details on the selection of materials, including WMA additives, base asphalt binders, and aggregate sources used in the present study. The description of the preparation of WMA blends has been presented. The experimental framework of the study has also been outlined.

This chapter, in addition, explores different aspects related to the ageing of WMA binders. The details of the ageing protocol proposed in this study have been provided. The methodology of the tests used for determining the surface morphology using scanning electron microscope and chemical interaction using Fourier transform infrared spectroscopy has been described. A brief description about the conventional tests, such as penetration value, softening point, and viscosity, has been given. The use of DSR for evaluating different rheological characteristics has been detailed, together with different techniques of analyzing and interpreting the rheological data. The working principle of accelerated tests, such as multiple stress creep and recovery (MSCR) and linear amplitude sweep test (LAST), has also been stated. Considering the performance of asphalt mixtures, the description of various test methods for characterizing the asphalt mixtures has been provided.

The results comprising the effect of WMA additives on the morphology, chemical interaction, and basic properties of the WMA binders have also been discussed and compared with the results of base asphalt binders.

3.2 Materials Used

3.2.1 Asphalt Binders

Asphalt binder is one of the mankind's oldest engineering material [446]. It has strong adhesive and waterproofing properties and is most widely used for the construction and maintenance of roads all over the world. It is manufactured from crude oil through a series of distillation techniques undertaken during petroleum refining [447]. Asphalt binder is a viscoelastic material whose properties are the function of both time and frequency/rate of loading [448]. It is the most important component in the asphalt mix and contributes significantly to the mechanical response to any given load and temperature conditions. The chemical composition of the asphalt binder is very complex in nature. It consists of carbon (82-88%), hydrogen (8-11%), sulfur (0-6%), oxygen (0-1.5%), nitrogen (0-1%), and traces of metals such as vanadium, nickel, magnesium, iron, and calcium [449,450]. The percentage of these constituents may vary depending on the type of crude oil and its source. Thus, in the present study, asphalt binders were collected from a single source to ensure consistency.

Two different base asphalt binders were used in this study to assess the effect of asphalt binder type on the properties of asphalt binder and mixtures. A viscosity graded (VG) asphalt binder, VG30, and a polymer-modified (PMB) asphalt binder, PMB40, were used. Basic tests were performed on these base asphalt binders in accordance with IS 73:2013 [451] and IS15462:2004 [452], and the results are shown in Table 3.1.

3.2.2 Aggregates

Aggregates are considered as the skeleton of the pavement structure. The properties of the aggregates vary with the change in their mineralogical source. Therefore, the

selection of aggregates necessitates careful assessment prior to construction work. Granite and dolomite aggregates (properties shown in Table 3.1) were used in the present study. Different sources were chosen to assess the effect of aggregate mineralogy on the properties of asphalt mixtures.

Table 3.1. Physical properties of asphalt binders and aggregates

Base Asphalt Binders					
Properties	**Test Methods**	**Obtained Results**		**Specified Limits**	
		VG30	**PMB40**	**VG30**	**PMB40**
Penetration value at 25°C, 0.1 mm	IS 1203 [453]	65	49	Minimum 45	30-50
Viscosity at 60°C for VG30 and 150°C for PMB40, Poises	IS 1206) [454]	2800	6.5	2400-3600	3-9
Kinematic viscosity at 135°C, cSt	IS 1206 [454]	406	-	Minimum 350	-
Flash point, °C	IS 1209 [455]	235	245	Minimum 220	Minimum 220
Solubility in trichloroethylene, %	IS 1216 [456]	99.8	-	99	-
Softening point, °C	IS 1205 [457]	50	70	47	60
Elastic recovery at 15°C, %	Annex A (IS 15462) [452]	-	78	-	70
Separation difference in softening point, °C	Annex B (IS 15462) [452]	-	2.1	-	Maximum 3
Aggregates					
Properties	**Test Methods**	**Obtained Results**		**Specified Limits**	
Combined flakiness and elongation index, %	IS 2386 (Part I) [458]	20	24	Maximum 35	
Los Angeles abrasion value, %	IS 2386 (Part IV) [459]	21	19	Maximum 30%	
Aggregate impact value, %	IS 2386 (Part IV) [459]	18.5	23	Maximum 24%	
Note: All the physical properties of the considered base asphalt binders and aggregate sources are within the specified limits.					

3.2.3 Warm Mix Additives

WMA is produced by adding certain additives to the asphalt binder or the asphalt mixtures [39,40]. These additives, referred to as WMA additives, can be broadly divided into three categories: a) Organic-based, b) Chemical-based, and c) Foaming-based. The details of the functioning of these technologies have already been discussed in chapter 1 (section 1.3).

Five different WMA additives with different dosages were used in the present study. The additives were chosen from different categories of WMA technologies, each having unique working mechanisms. Sasobit (S) and Sasobit Redux (SR) (characterized under organic-based category); Cecabase RT Bio 10 (C) and Rediset LQ1102CE (R) (characterized under chemical-based category); and Aspha-Min (Am) (from foaming-based category) were selected. Figure 3.1 (a-e) shows the visual appearance of each WMA additive. The dosages were chosen based on manufacturer recommendations. The basic description of the selected WMA additives is provided in Table 3.2. The qualitative and quantitative properties of the additives are given in Table 3.3.

(a) (b)

(c)

(d)

(e)

Figure 3.1. WMA additives (a) Sasobit, (b) Sasobit Redux, (c) Cecabase, (d) Rediset, and (e) Aspha-Min

Table 3.2. Description of warm mix additives adopted in this study

Technology	Product/Additive	Company	Description	Dosage(s) Used
Organic	Sasobit	Sasol [460]	Aliphatic synthetic paraffin wax produced from the Fischer-Tropsch method	1%, 2%, 3.0% w/b

Organic	Sasobit Redux	Sasol [461]	Aliphatic synthetic paraffin wax produced with the use of Fischer-Tropsch process	0.7%, 1.35%, 2.0% w/b
Chemical	Cecabase RT Bio 10	Ceca (Arkema) [462]	Bio-sourced cationic surfactant	0.2%, 0.35%, 0.5% w/b
Chemical	Rediset LQ1102CE	Nouryon (formerly Akzo Nobel) [463]	Cationic surface-active agent	0.4%, 0.5%, 0.6% w/b
Foaming	Aspha-Min	MHI [464]	A foaming process with synthetic zeolite	0.3% w/m

Note: w/m and w/b indicate by weight of the asphalt mixture and by weight of the asphalt binder, respectively.

Table 3.3. Qualitative and quantitative characteristics of selected warm mix additives

Properties/Technologies		**Organic**		**Chemical**		**Foaming**
		Sasobit [460]	**Sasobit Redux** [465]	**Cecabase RT Bio10** [462]	**Rediset LQ1102CE** [463]	**Aspha-Min** [464]
Qualitative	**Ingredients**	Long-chain aliphatic hydrocarbon	Long-chain aliphatic hydrocarbon	Fatty alcohol derivates	Poly Fattiamines	80% sodium aluminum silicate and 20% water
	Odor	Odorless	Odorless	NA	Amine-like	Odorless
	Physical State	Pellets	Pellets	Liquid	Clear Liquid	Granular powder
	Visual colour	White	White	Brown	Pale Yellow	White to grey
Quantitative	**Density at room temperature (g/cm^3)**	0.59-0.62	0.79	0.99-1.01	1.00	0.5-0.6

	Flash Point (°C)	285	240	174	165	NA
	Melting Point (°C)	85-110	70-83	NA	0	>1200
	Solubility in water	Insoluble	Insoluble	Insoluble, forms a colloidal solution	Partially soluble	Insoluble
	pH value	Neutral	Neutral	10	NA	11-12

Note: NA indicates Not Available.

3.2.4 Preparation of WMA Binders

To prepare WMA binders (organic and chemical-based), base asphalt binders were heated using a temperature-controlled heating mantle until they became fluid enough to be poured. 500 gm of base asphalt binders were taken and appropriately stirred to remove the entrapped air. After that, the selected dosages of the WMA additives were added to the preheated base asphalt binders. Mixing was commenced using a high-shear propeller mixer (as shown in Figure 3.2a) operated at a speed of 500 rpm. In the case of VG30, mixing was continued for 30 minutes under a controlled temperature range of 130-140°C. For PMB40, mixing was done in two stages. The first stage involved the stirring of base PMB40 for 15 minutes to ensure proper dispersion of polymers within the asphalt binder, followed by the second stage, wherein the blending with WMA additives was done for 30 minutes at a temperature of 140-150°C. The blending time, speed of high shear mixer, and temperatures were selected based on the past studies [246,466,467]. To ensure equivalent ageing conditions during the mixing process, VG30 and PMB40 were also subjected to the same mixing protocol (as adopted for respective WMA binders) prior to testing. For foaming-based technology, Aspha-,Min was directly added during the mixing of asphalt binders and aggregates i.e., during the

production of asphalt mixture, as shown in Figure 3.2b. Therefore, preparation of modified asphalt binders was not required in this case. Table 3.4 shows the terminology (used in chapter 3 and 4) for different combinations of WMA additives and asphalt binders.

Table 3.4. Terminology used in the present study

WMA additives with their dosage	**Labels corresponding to base asphalt binders**	
	VG30	**PMB40**
No additive	VG30	PMB40
1% Sasobit	S1	PS1
2% Sasobit	S2	PS2
3% Sasobit	S3	PS3
0.7% Sasobit Redux	SR0.7	PSR0.7
1.35% Sasobit Redux	SR1.35	PSR1.35
2% Sasobit Redux	SR2	PSR2
0.2% Cecabase	C0.2	PC0.2
0.35% Cecabase	C0.35	PC0.35
0.5% Cecabase	C0.5	PC0.5
0.4% Rediset	R0.4	PR0.4
0.5% Rediset	R0.5	PR0.5
0.6% Rediset	R0.6	PR0.6
0.3% Aspha-Min	Am	PAm

Note: All the WMA additives were added by weight of asphalt binder, except Am. Am was added directly to the mix at a rate of 0.3% by weight of the asphalt mixture as per the manufacturer recommendation.

Figure 3.2. Stepwise preparation of WMA binder and mixtures (a) organic and chemical-based WMA binders and (b) foaming-based WMA mixture

3.2.5 Ageing Condition

Asphalt binder (or asphalt mixture) is subjected to a series of complex physiochemical progressions, including oxidation, polymerization, syneresis, volatilization, evaporation, dehydrogenation, condensation, steric hardening, and many more, leading to the embrittlement/hardening of asphalt binder. This hardening phenomenon is termed ageing [76,468]. It is a complex phenomenon, which contributes to the premature failure of the asphalt pavements. Ageing in asphalt mixture can be broadly characterized into two stages: short-term ageing (STA) and long-term ageing (LTA). STA is caused during the production, transportation and paving of asphalt mixtures. On the other hand, LTA occurs due to the progressive oxidation of the asphalt mixture

throughout its service life [469]. As an organic material, asphalt binder undergoes changes in its micro-structure, chemical composition, and mechanical behavior due to the effect of ageing during the in-service life. Figure 3.3 provides insights on variation in the stiffness of the asphalt binder with time due to the typical effect of ageing. As can be seen, STA occurs at a very rapid rate, whereas LTA evolves with time at a lower rate.

Asphalt binders/mixtures are subjected to STA and LTA in the laboratory for a short period of time, through the application of heat and air, to replicate the field ageing. In general, the effect of STA and LTA can be simulated at two different levels in asphalt binder and in asphalt mixture. The details of both the ageing procedure adopted in this study are described below:

3.2.5.1 Ageing of Asphalt Binders

A rolling thin film oven (RTFO) and pressurized ageing vessel (PAV) methods are conventionally used to simulate STA and LTA of asphalt binders, respectively. However, several other test methods have been proposed in the literature to simulate the ageing of asphalt binders. In the present study, the ageing was simulated using the Universal Simple Ageing Test (USAT) procedure developed by Western Research Institute (WRI) [470]. USAT utilizes a draft oven for ageing the asphalt binder as it is simple and convenient. Farrar et al. [470] demonstrated that the attributes (ageing time, ageing temperature, and pressure) used in USAT directly simulate STA and LTA obtained by RTFO and PAV method, respectively. These methods have been successfully adopted in previous researches[471–477]. The in-depth details on the adopted ageing method can be found elsewhere [470].

A part of the prepared samples (base binders and WMA binders) were subjected to ageing conditions. Initially, the asphalt binders were spread in the flat dish plate to a very thin film thickness (300 μm) using a spatula. The dish plate was further kept inside the draft oven for a fixed time and temperature condition. Farrar et al. [470] recommended conducting the STA of asphalt binders at a fixed temperature of 150°C (HMA) and 130°C (WMA) for a period of 50 minutes. The temperature of 150°C and 130°C were selected in Farrar's study because the average mixing temperatures of all the HMA and WMA binders were around 150°C and 130°C, respectively. Since the present study involves the application of WMA technology, wherein the asphalt mixtures are produced at lower temperatures relative to conventional HMA mixtures, it is obvious that STA of WMA binders would occur at relatively lower temperatures. Thus, in this study, the asphalt binders were aged at their corresponding mixing temperatures, using the approach specified in Farrar et al. [470], to simulate the STA in a more generic way. STA samples were further subjected to LTA conditions following Farrar et al. [470]. Here, the temperature corresponding to LTA was not altered and kept the same for HMA and WMA binders, as both binders are subjected to similar field exposure throughout their service life. The whole process of simulating STA (modified protocol) and LTA of asphalt binders is shown in Figure 3.3.

After the ageing process, the asphalt binders were cooled and scrapped using a scrapping tool. The asphalt binders in unaged condition (UA), STA condition, and LTA condition were stored in separate containers for further experimentation.

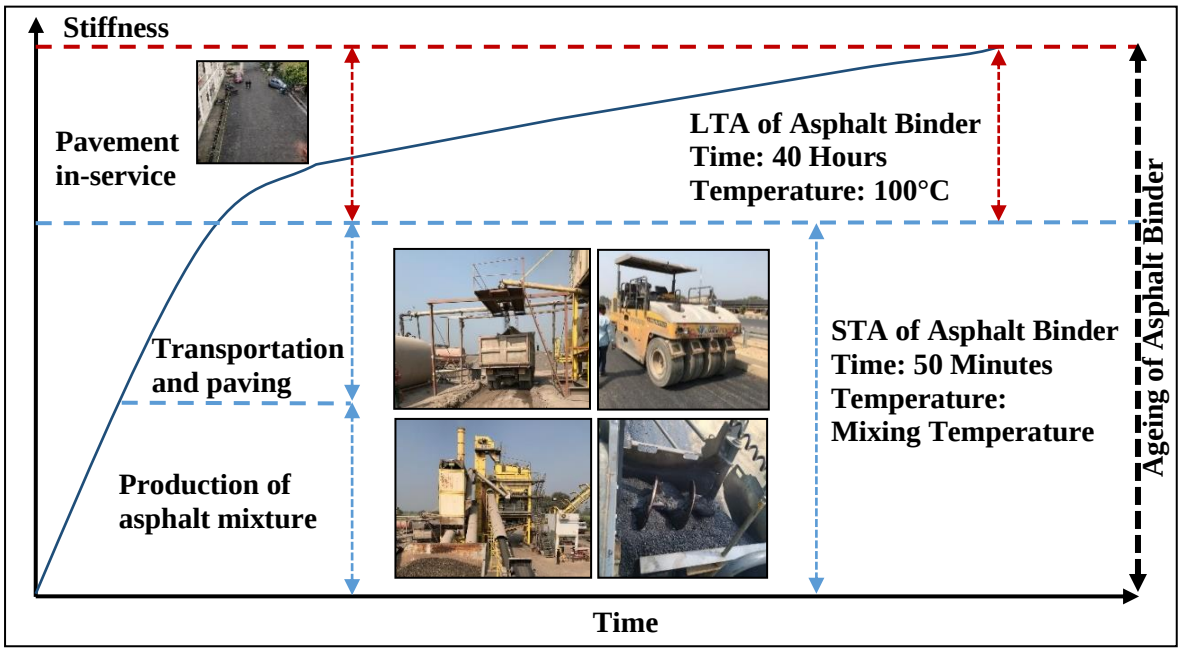

Figure 3.3. STA and LTA of asphalt binders

3.2.5.2 Ageing of Asphalt Mixtures

Though a considerable amount of research work has been done on simulation of ageing for asphalt binders, the ageing of asphalt mixtures has not been explored with enough rigor. Generally, AASHTO R30 [478] is followed to simulate the ageing of asphalt mixtures in the laboratory. As per the standard, ageing should be carried out in a forced draft oven for a specified time and temperature, depending on the type of ageing condition. Table 3.5 shows a brief description of different types of ageing conditions, as per AASHTO R30 [478]. It is debated that the specified protocols are not suitable for asphalt mixtures produced using technologies, such as PMB, reclaimed asphalt pavement materials (RAPM), and WMA. For example: since WMA mixtures are produced and compacted at lower temperatures, there is a lower impact of temperatures on ageing as well as absorption of asphalt binder by the mineral aggregates. As would be expected, the WMA binder, conditioned at lower compaction temperature, is less stiff than the conventional HMA binder. In addition, the high ageing temperature (as

per AASHTO R30 approach [478]) for WMA may indicate false performance results. In this study, the method proposed in NCHRP 815 (project 09-52) [479] was used to simulate the STA of asphalt mixtures. NCHRP approach considers a wide range of variables, including binder type, aggregate source, WMA technology, RAPM, production temperatures, etc, to select a suitable protocol that directly simulates the field ageing that occurs during the production, placement and compaction stages. The STA of asphalt mixtures was simulated by conditioning the loose asphalt mixture (as shown in Figure 3.4a) at their respective compaction temperature for a period of two hours, irrespective of the mixture type. This approach/protocol was followed regardless of whether the mixture being produced for volumetric or performance evaluation. To simulate the LTA of asphalt mixtures in the laboratory, STA conditioned loose asphalt mixtures were further compacted and subsequently subjected to a draft oven (Figure 3.4b) at a temperature of 85°C for five days in accordance with AASHTO R30 [478]. The whole process of STA and LTA of asphalt mixtures [480], along with the adopted protocol, is explained pictorially in Figure 3.5.

Table 3.5. Different types of conditioning as per AASHTO R30 [478]

Type of Conditioning	**Simulation**	**Time, hours**	**Temperature, °C**
Volumetrics	Absorption of asphalt binder	2	Compaction Temperature
STA	Production and construction	4	135
LTA	After construction process till failure approach	120	85 (on STA compacted samples)

(a) (b)

Figure 3.4. Simulation of ageing in laboratory using forced draft oven (a) STA on loose asphalt mixtures and (b) LTA on compacted asphalt mixtures

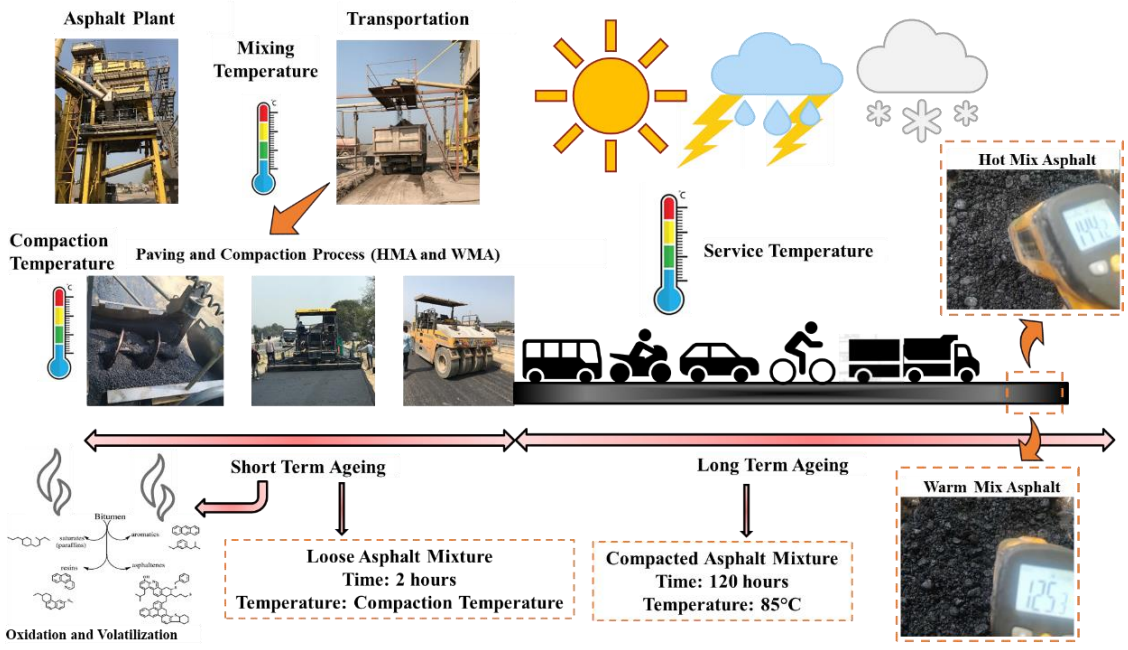

Figure 3.5. Complete process indicating STA and LTA of asphalt mixtures

3.3 Experimental Framework

A series of experimental testing's and theoretical analysis have been performed to understand the efficacy of WMA technology for pavement construction. Initially, various tests were commenced to characterize the materials used in the present research work. These characterization tests include the morphological observations of asphalt binders, chemical interaction between WMA additives and asphalt binders, and basic experimental tests such as penetration, softening point, viscosity, and high-temperature performance grading (PG). Following the material characterization, different techniques were used to evaluate the mixing and compaction temperatures of HMA and WMA mixtures. The appropriate/reliable method was selected, and subsequently, the obtained mixing and compaction temperatures were validated using different approaches. Thereafter, the optimum dosage of WMA additives, pertaining to different technologies, was assessed. After selecting the optimum dosage, the performance-based testing and analysis were carried out on the asphalt binders and mixtures prepared using the optimum dosage of WMA additives. All these tests and analysis were performed by taking base asphalt binders (VG30 and PMB40) and conventional HMA (VG30 and PMB40) as the reference asphalt binders and mixtures, respectively. Since Aspha-Min (a foaming-based technology) was directly added during the preparation of asphalt mixtures, the testing and analysis of Aspha-Min inclusive asphalt binders have not been conducted or not taken into consideration throughout the investigation of asphalt binders. Figure 3.6 shows the outline of the research work executed in this study.

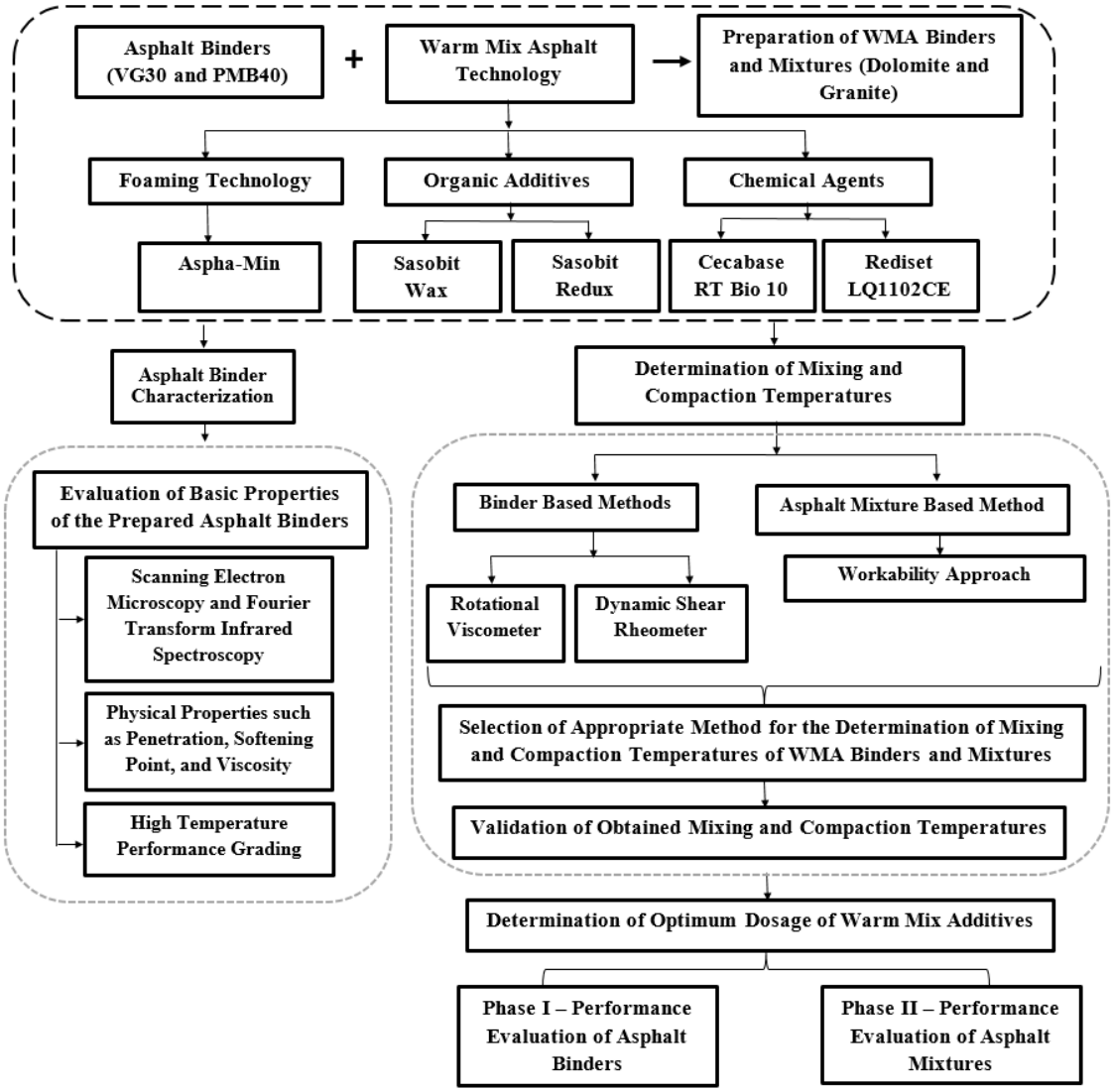

Figure 3.6. Outline of the research work

The performance-based testing of prepared asphalt binders and mixtures was assessed in two phases. The first phase involved the performance evaluation of asphalt binders, whereas the second phase included the performance evaluation of asphalt mixtures. The performance of WMA binder and mixtures were ascertained by conducting various tests, using the experimental framework shown in Figure 3.7a and Figure 3.7b, respectively. The tests were carried out on UA, STA, and LTA conditioned asphalt binders and mixtures, based on the requirement of the test method, as per the standard

specifications. The rheological tests were performed using Anton Paar (SmartPave) MCR 102 Dynamic Shear Rheometer (DSR). The silicone mold method was used to prepare the test specimens [481]. All the tests were performed thrice, and the average of obtained results are presented in this study. It was found that the coefficient of variation for all the measurements was under 10%.

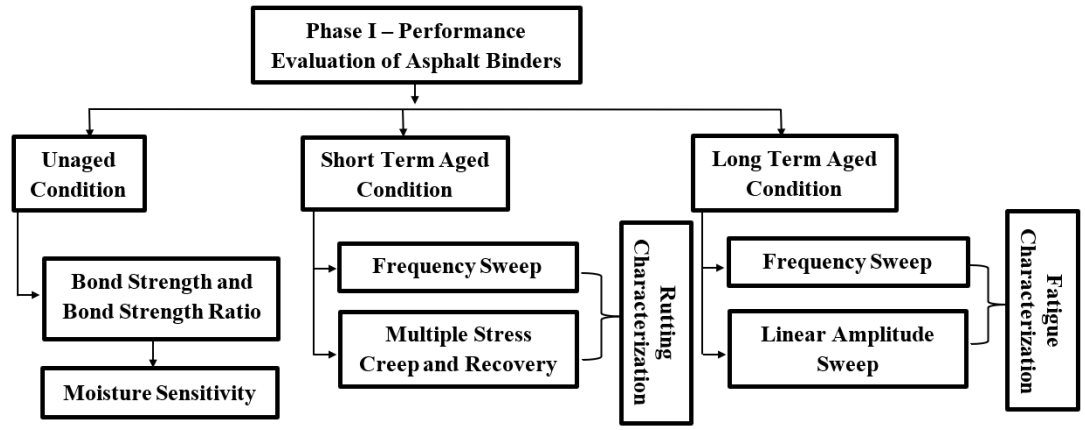

(a)

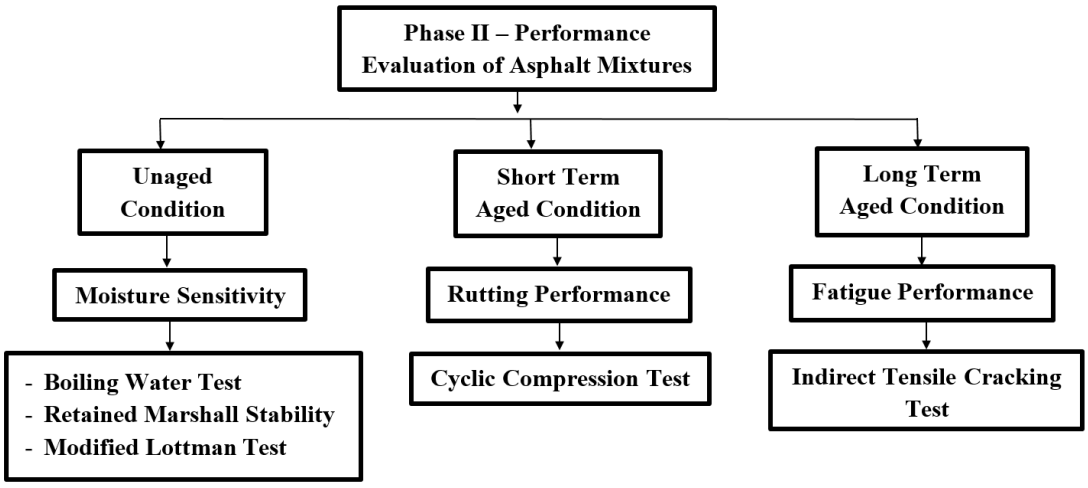

(b)

Figure 3.7. Experimental framework (a) Phase 1 and (b) Phase 2

3.4 Methodology

3.4.1 Basic Characterization of Asphalt Binder

The discussion on the basic characterization of VG30, PMB40, and corresponding WMA binders is described in the subsequent sections:

3.4.1.1 Scanning Electron Microscopy

SEM is an essential tool that can observe and analyze the surface texture of any material on a micrometer to nanometer scale. SEM works on the principle of emitting a high-energy electron beam on the surface of any given material (here asphalt binder) and converting the obtained information (secondary electron and backscattered electron) into electric signals through the use of a scan generator and amplifier. The converted signals are further digitized, stored, processed and displayed transparently in an image form using SEM analysis software. Figure 3.8 shows the schematic representation of the working principle of SEM.

The test procedure in SEM causes excessive accumulation of electrons on the surface of the asphalt binder under the electron beam to create an image. This accumulation of electrons leads to surface charging that can distort SEM images. To avoid this, the samples are generally coated with a thin film (<10 μm) of gold and palladium alloy, using a sputter coating process (Figure 3.9a). The thickness of the film is so small that all the microstructural aspects at the surface of the asphalt binder are preserved, and no noise in images is created during the scanning process (Figure 3.9b). The sputter coating process also lowers the vacuum level inside the chamber, which introduces conductivity to the surface of the asphalt binders prior to SEM observation. This helps in neutralizing the accumulation of electrons, thereby removing the effect of charging. The surface morphology and microstructural analysis of the asphalt binders were conducted using

an EVO-SEM MA15/18 (Carl Zeiss Company Ltd.) scanning electron microscope (SEM), as shown in Figure 3.9c.

The SEM was operated at an accelerating voltage of 20 kV to examine dispersion and quantify the efficacy towards the blending process. For each sample, the images were taken at magnification levels of 50×, 100×, 200×, 500×, 2k×, 3kx, 5k×, and 10k×. However, the discussion provided in this study corresponds to 5 K×. Figure 3.9d shows an example of a typical SEM image taken at a magnification level of 5K×.

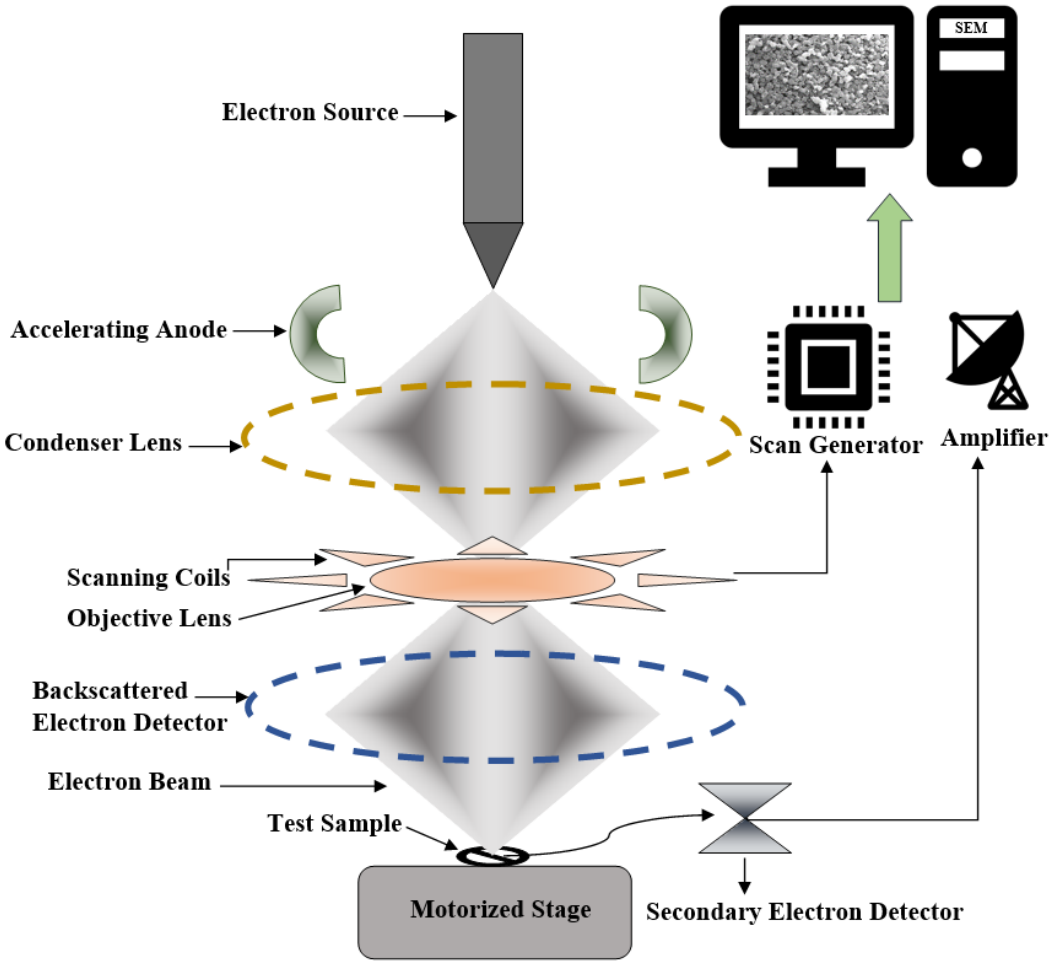

Figure 3.8. SEM principle

(a)

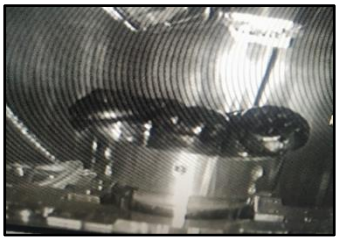

(b)

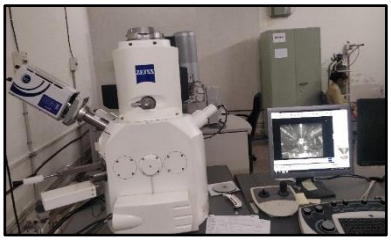

(c)

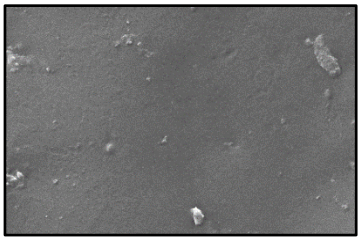

(d)

Figure 3.9. Process of Scanning electron microscopy (a) Sputter coating, (b) Coated sample inside EVO-SEM, (c) EVO-SEM machine, and (d) Typical SEM image

3.4.1.1.1 Discussion on SEM Observations

It is essential to understand the interaction of WMA additives at the micro-level, as it is directly associated with the performance of asphalt binders and mixtures at the macro level. SEM analysis was carried out to observe the micromorphology and the interaction (dispersion) characteristics of WMA additives within the asphalt binders. These characteristics are a function of several factors, including temperature and time of blending, shear rate, WMA technology, and their respective dosage. Therefore, in the present study, blending time, temperature, and shear rate were kept the same to adjudge only the effect of WMA additives on the morphological and dispersion characteristics of the chosen base asphalt binders.

Figure 3.10a and Figure 3.10b present the SEM images of VG30 and PMB40 respectively, corresponding to the zoom rate of 5K×, of VG30 and PMB40, respectively. As can be seen, both the base asphalt binders showed a clear, uniform and

continuous phase over the surface. Figures 3.11 and 3.12 show that WMA additives, irrespective of WMA technology and dosages, were uniformly dispersed and distributed throughout the asphalt binder matrix. The inferences obtained from SEM images revealed that the mixing technique adopted in this study was effective for homogeneous/uniform blending of different WMA additives within the asphalt binder, irrespective of the base binder. However, the surface morphology of each WMA binder varied with the type of WMA technology. This can be attributed to the difference in the physical form of WMA additives; for example, organic-based additives, used in this study, were in pellets form, whereas the physical state of both the chemical agents was liquid. The change in surface morphology with WMA additives is also a function of the base asphalt binder. Thus, it is speculated that different WMA additives would affect the performance differently, depending on the type of base asphalt binder. The effect of different WMA additives and their dosages on the surface morphology of VG30 and PMB40 are discussed in the next section.

Effect of WMA technologies on the morphology of VG30

The addition of organic-based additives, viz. Sasobit and Sasobit Redux, lead to the formation of crystallized pellet structure over the surface of asphalt binder, as depicted in Figure 3.11 (a-f). Though a bitumen-rich phase was observed at lower dosages of Sasobit and Sasobit Redux, the increase in dosage (from S1 to S2 or S3, and SR0.7 to SR1.35 or SR2) proportionately changed the surface morphology. A high dosage of Sasobit and Sasobit Redux clearly indicated a crystal-rich phase scattered throughout the surface. However, the surface pellets in Sasobit Redux modified asphalt binder were observed to be more integrated and smoother than the rough pellet surface of Sasobit-based asphalt binders, irrespective of the dosages. In addition, the crystals of Sasobit in VG30 adhered together to form a thin crosslinking crystallized network (Figure 3.11b

and Figure 3.11c), whereas no such network appeared in Sasobit Redux-based WMA binders. This is attributed to the fine crystalline long-chain aliphatic hydrocarbon in Sasobit (40-115 carbon atoms) compared to Sasobit Redux (15-65 carbon atoms). The hydrocarbon length of Sasobit Redux is comparatively similar to conventional asphalt binders (22-45 carbon atoms), thereby resulting in similar melting point. The observations of the present study appreciably support the inferences of the past researchers [92], who reported that organic waxes combine with asphalt binder and influence their hydrocarbon chain length. These attributions indicate that organic-based WMA additives might lead to the change in physical, rheological, and mechanical properties of asphalt binders and mixtures. Since, the hydrocarbon length of Sasobit Redux is comparatively similar to conventional asphalt binders (22-45 carbon atoms), it is expected that the addition of Sasobit Redux will not contribute to the change in physical properties of asphalt binders.

Chemical agents, on the other hand, showed different surface characteristics than organic-based WMA additives. The addition of Cecabase in VG30 resulted in a wrinkled surface with warped sides. However, this appearance was only noticed at a lower dosage of Cecabase (particularly at 0.2% dosage) (Figure 3.11g), while a uniform dispersion was identified with other dosages (Figure 3.11h and Figure 3.11i). Such wrinkled surface characteristics or warping effect were not found in Rediset-based WMA binders; rather an intact microstructure of small crystals was observed, irrespective of the dosage. Rediset, added in liquid form, was observed to be homogeneously dispersed and embedded in VG30 with a clear crystal boundary (Figure 3.11 (j-l)). At R0.5 and R0.6, as shown in Figure 3.11k and Figure 3.11l, respectively, the crystals become agglomerated, indicating a sharp periphery. This confirmed the poly-functional behavior of Rediset, signifying a combination of cationic surfactant and

organic-based rheology modifier. The surfactant part allows the uniform dispersion of the additive, whereas the organic part aid in the crystallization effect (indicated by the coarse surface structure). The morphological observation showing synergistic effect in Rediset additive at the micro-scale could further influence the performance of asphalt binders and mixtures at the macro level. Overall, these additives (Cecabase and Rediset) act at the microscopic interface of the asphalt binder and aggregate system and thereby influence the viscoelastic behavior [92].

Effect of WMA technologies on the morphology of PMB40

Figure 3.12 (a-l) shows the SEM images of different WMA binders (at varying dosages) prepared with PMB40 as a base asphalt binder. Alike VG30, the microstructure of PMB40 appears to be a single-phase uniform structure. Although the addition of Sasobit in VG30 led to a crystallized structure over the surface, no noticeable change was observed in the case of PMB40. This is attributed to the dominance of the high carbon crosslinking network formed by the polymers present within the composite. However, some segregated patches of crystalline waxy particles were identified at a higher dosage of Sasobit (i.e., S3), as depicted in Figure 3.12c. Unlike Sasobit, the incorporation of Sasobit Redux significantly affected the surface morphology of PMB40, but the change was a function of the dosage of the additive. At a lower dosage (i.e., SR0.7), Sasobit Redux tries to intercalate within the strong polymeric network of PMB40 (Figure 3.12d). An increase in dosage of Sasobit Redux from 0.7% to 1.35% might have resulted in the formation of a fragmented dendritic microstructure, as observed in Figure 3.12e. This dendrite structure may be originated due to the increased waxy concentration in the polymer-rich phase of PMB40, which further becomes much denser with an increased dosage of Sasobit Redux. In the SEM image of SR2, as shown in Figure 3.12f, a dense fine-crystal-like structure was seen, indicating the overlapping

of the wax-rich phase over the polymeric network of PMB40. The conversion from a polymer-rich phase to a waxy phase, at a higher dosage of Sasobit Redux, maybe due to the destruction of equilibrium between the dispersed phase (SR2) and dispersion medium (PMB40).

The addition of Cecabase in PMB40 led to the creation of a rugged and layered interconnecting structure with a coarse surface. With C0.5 (Figure 3.12i), a uniformly dispersed and thick patch-like layered structure was observed over the surface of the asphalt binder. This phase generally aids in improving the wettability and coating of aggregate. On the other hand, the incorporation of Rediset in PMB40 resulted in clustered, lapped, or jointed structure, depending on the additive dosage, as depicted in Figure 3.12 (j-l). Interestingly, a crack arresting effect was observed with the addition of 0.6% Rediset (Figure 3.12l). One possible interpretation for this discrete behavior is the poly-functioning of Rediset, which affects the surface morphology of PMB40 and eventually the performance as well. Unlike organic-based additives in PMB40, the morphology of chemical based WMA binders varied with the change in dosage.

Based on the SEM observations, it is concluded that all the WMA additives indicate a definite impact on the surface morphology of the base asphalt binders (VG30 and PMB40). This leads to the speculation that WMA additives, irrespective of their type and dosages, may also influence the performance of asphalt binders and mixtures on a macro-scale.

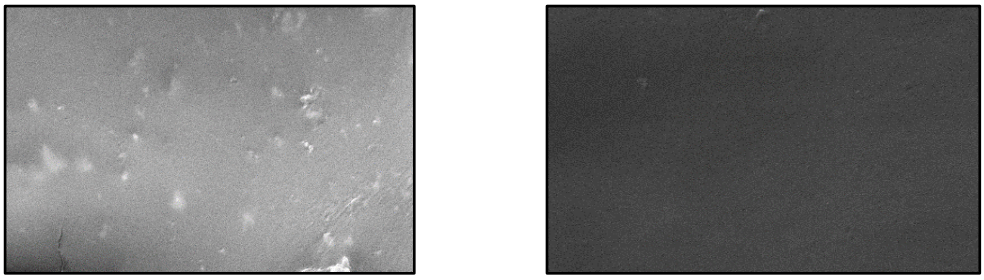

(a) (b)

Figure 3.10. SEM images (a) VG30 and (b) PMB40

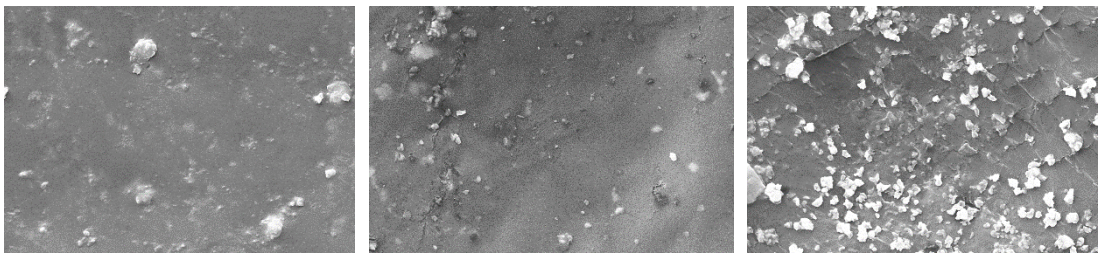

(a) (b) (c)

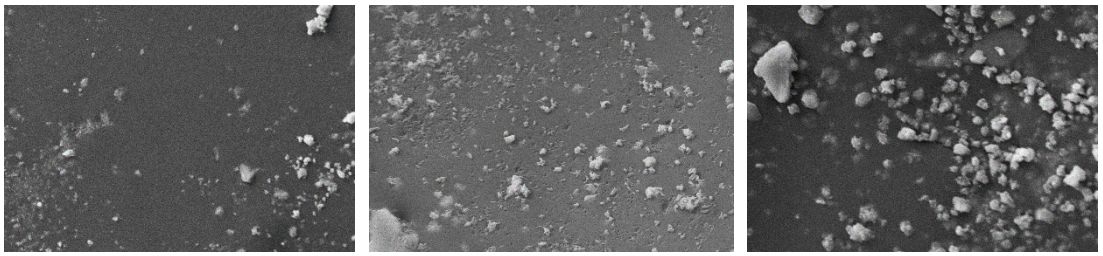

(d) (e) (f)

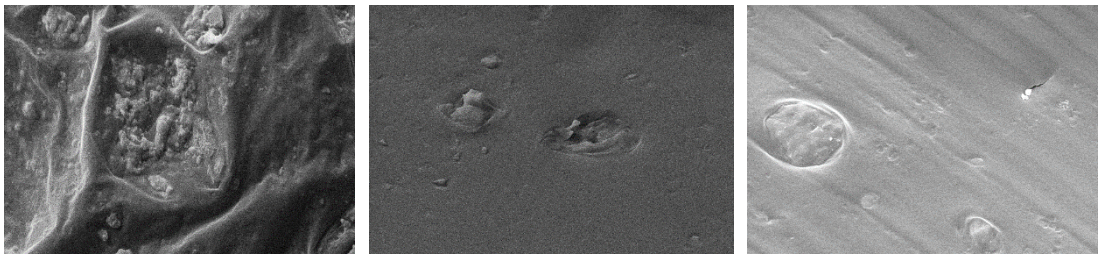

(g) (h) (i)

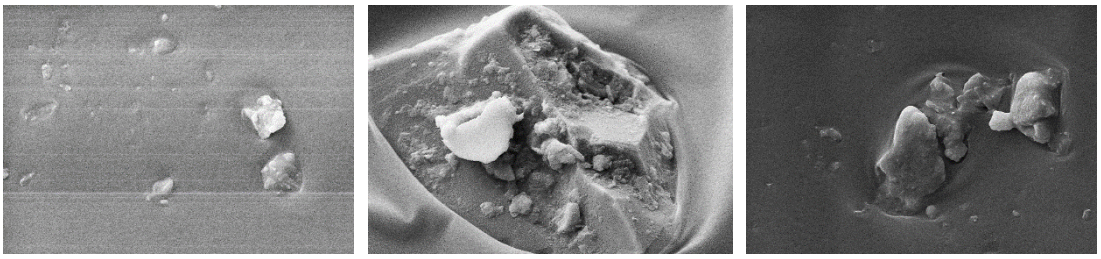

(j) (k) (l)

Figure 3.11. SEM images of WMA binders prepared with VG30 (a) S1, (b) S2, (c) S3, (d) SR0.7, (e) SR1.35, (f) SR2, (g) C0.2, (h) C0.35, (i) C0.5, (j) R0.4, (k) R0.5, and (l) R0.6

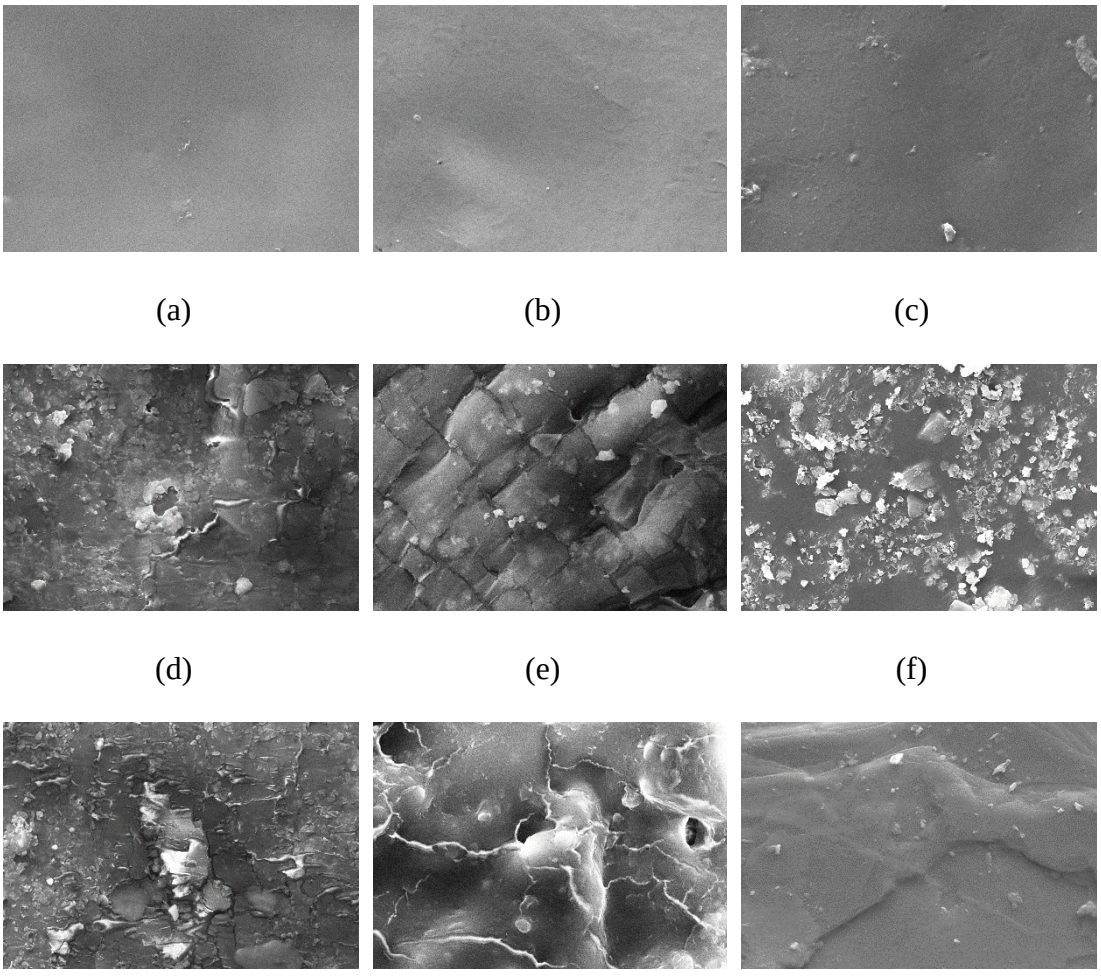

(a) (b) (c)

(d) (e) (f)

(g) (h) (i)

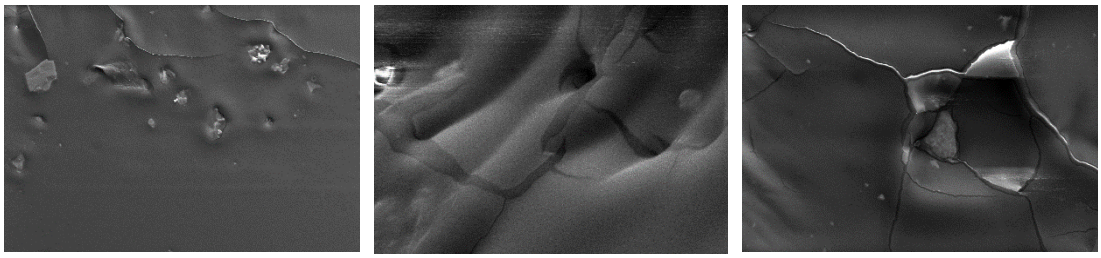

(j) (k) (l)

Figure 3.12. SEM images of WMA binders prepared with PMB40 (a) PS1, (b) PS2, (c) PS3, (d) PSR0.7, (e) PSR1.35, (f) PSR2, (g) PC0.2, (h) PC0.35, (i) PC0.5, (j) PR0.4, (k) PR0.5, and (l) PR0.6

3.4.1.2 Fourier Transform Infrared Spectroscopy (FTIR)

FTIR is a fast and reliable technique for identifying/quantifying the variation in chemical constituents (functional groups) in any material [76]. FTIR works on the principle that a given material (here, asphalt binder) absorbs infrared radiation at specific frequencies that are characteristic of its structure. FTIR method collects the interferogram of any given material using an interferometer (beam splitter). An interferogram is a pattern of waves generated by making measurements of the received radiations at different positions using a fixed and movable mirror. These radiations are further passed through the sample, which causes vibration in the molecular bond at discrete frequencies, and results in absorbance or transmittance of the radiations based on their directions [214]. Thereafter, an FTIR spectrometer digitizes the collected interferogram and subsequently performs the Fourier Transform function to display the actual spectrum. An FTIR spectrometer simultaneously accumulates the high-resolution spectral data over a wide spectral range (wavenumber) [218]. In this study, these widespread spectrums were examined to detect the change in functional groups with the addition of WMA additives in the base asphalt binders. Figure 3.13 shows the schematic overview of the working principle of FTIR.

In the present study, Nicolet iS5 FTIR spectrometer with iD1 transmission accessory was used to analyze the asphalt binders. The potassium bromide (KBr) pellet method was adopted owing to the transparency of KBr in the infrared region selected in this study (i.e., 500 cm^{-1}~2000 cm^{-1}) [218]. In addition, KBr is more compatible with organic materials and was found to be an excellent refractive index for identifying the functional groups in asphalt binders with greater resolution. As per this method, a very small amount of asphalt binder was taken and mixed thoroughly with dry KBr powder, using a mortar and pestle. The mixed composite was then filled in a pellet die, as shown using the arrow in Figure 3.14a, and pressed under a hydraulic pellet press machine (Figure 3.14b) at a pressure of 100 kg/cm^2. Next, the pressed thin cylindrical sample was removed from the die and subjected to an FTIR sample holder attached to the spectrometer (Figure 3.14c) to identify the chemical constituents. Measurements were taken with 32 scans at a resolution of 4 cm^{-1} over a wavenumber ranging from 500-2000 cm^{-1} and are shown in the form of absorbance (Figure 3.14d). Absorbance is the unit often used to measure the total amount of infrared radiation absorbed by any material.

Various research studies have used the FTIR technique to study the ageing behavior of asphalt binders. More specifically, it was reviewed that ageing causes the transformation of generic constituents (i.e., maltenes) into high molecular weight fractions (i.e., asphaltenes). This may lead to chemical changes within the asphalt binder functional groups, such as carbonyl and sulfoxide, corresponding to 1700 cm^{-1} and 1030 cm^{-1}, respectively [468,482]. To analyze the impact of WMA additive on the ageing characteristics, FTIR was conducted on UA, STA, and LTA conditioned asphalt binder samples. The absorbance peak corresponding to carbonyl (1700 cm^{-1}), and sulfoxide (1030 cm^{-1}) functional groups were analyzed and compared. In general, the

increase in the amount of carbonyl or sulfoxide bonds reflect a higher ageing effect. The results and discussions on the ageing characteristics of different asphalt binders are presented in chapter 5.

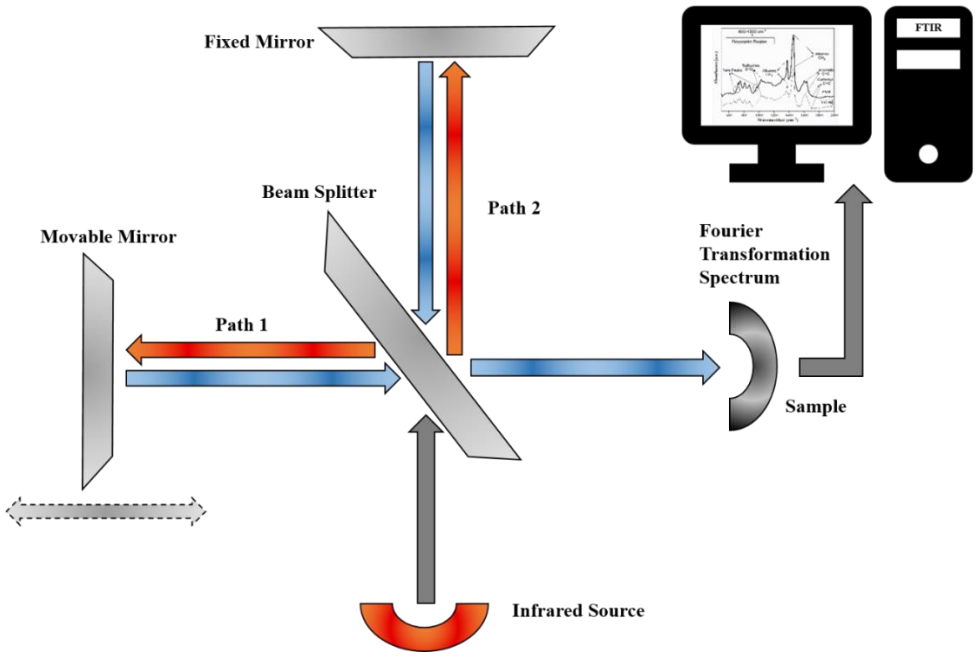

Figure 3.13. FTIR principle

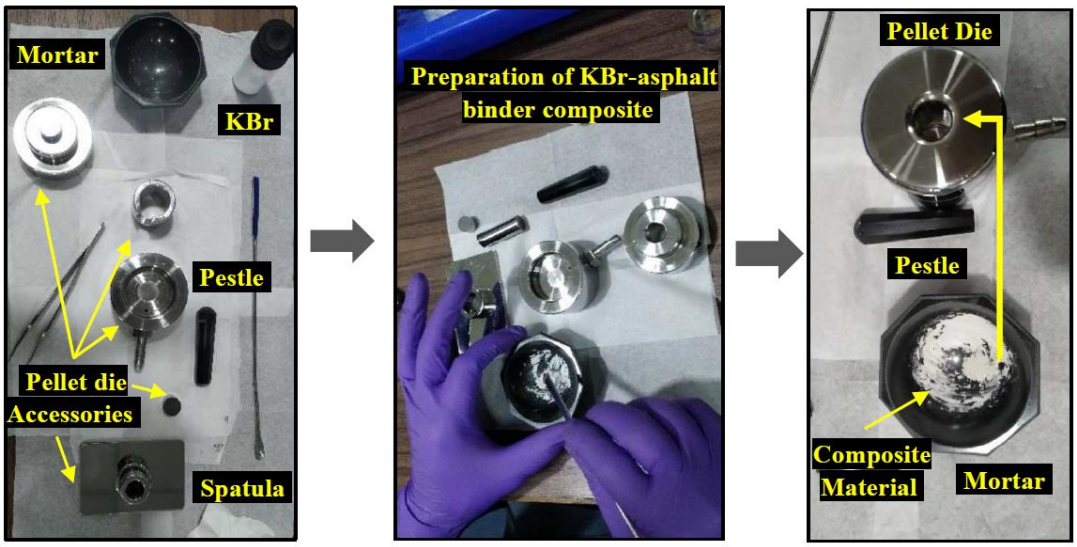

(a)

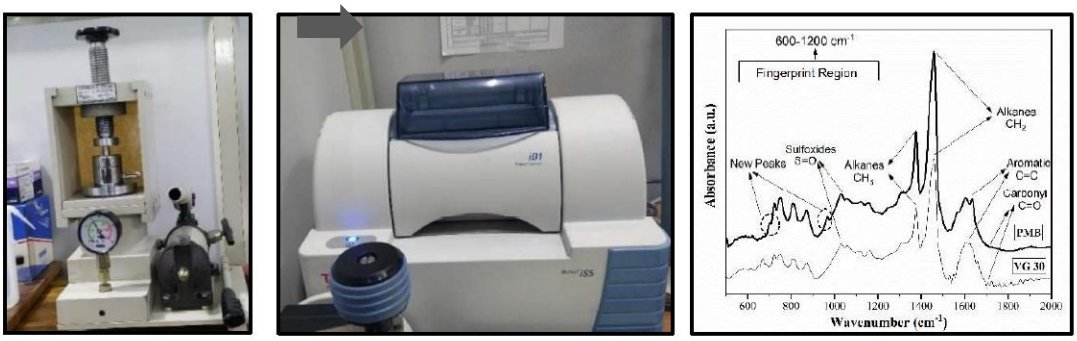

(b) (c) (d)

Figure 3.14. Process of FTIR (a) Preparation of sample for FTIR along with required accessories, (b) Hydraulic pellet press machine, (c) Nicolet iS5 FTIR spectrometer with iD1 transmission accessory, and (d) Typical FTIR spectrum data

3.4.1.2.1 Discussion on FTIR Spectral Analysis

FTIR spectral analysis is usually carried out to identify the functional group or chemical composition present within the asphalt binder. Figure 3.15 (a-b) presents the FTIR spectra of VG30 and PMB40. Several peaks, at specific wavenumbers, were observed for both the base asphalt binders. In general, all the peaks signify their own functional group with a definite molecular structure. The absorption band ranging from 2000-1200 cm^{-1} represents stretching vibration, including symmetric and asymmetric vibration [483,484]. This range of wavenumbers reflects the functional group for asphalt binder characterization. On the other hand, the absorption band ranging from 1200-600 cm^{-1} indicates the fingerprint region [485]. The fingerprint region plays a vital role in Squantifying the structure of the asphalt binder as it comprehends a very complex series of absorbance specifying bending vibrations, which are often difficult to interpret.

As shown in Figure 3.15a, irrespective of the base asphalt binders (VG30 and PMB40), the sharp peak at 1600 cm^{-1} was ascribed to the C=C alkene stretching vibration in aromatics. The peak of bending vibrations was identified near 1460 cm^{-1}, and 1374 cm^{-1}, where the first peak is associated with the asymmetric bending in CH_3 and scissors of

CH_2 and the later peak corresponds to the symmetric bending of CH_3 alkyl group, respectively[486]. These observed peaks were expected as asphalt binder ideally composed of long-chain hydrocarbon, including 82-88% carbon along with 8-11% hydrogen. Few valuable absorbance peaks were detected around 1700 cm^{-1} and 1030 cm^{-1} wavenumbers. These peaks correspond to carbonyl (C=O) and sulfoxides (S=O) functional groups, respectively [486], which are commonly used to quantify the degree of ageing in asphalt binders. A group of bulging peaks attributed to the rocking of long-chain CH_n, which comprises more than four carbon atoms in a row, was observed around 724 cm^{-1}. Generally, the peaks observed within the range of 700-900 cm^{-1} were due to the presence of =C-H in-plane bending vibration in aromatics and olefins [487].

While comparing VG30 and PMB40 spectrums, two new peaks, corresponding to wavenumbers 967 cm^{-1} and 698 cm^{-1}, were observed in PMB40 FTIR spectra (as shown using callouts in Figure 3.15b). The marked peak at 967 cm^{-1} indicated the presence of trans-disubstituted –CH=CH= of butadiene block, while the peak at 698 cm^{-1} resembled the wagging of C-H in trans-alkene (out of plane). Both these peaks (967 cm^{-1} and 698 cm^{-1}) are the prime chemical attributes of PMB 40, as they do not have any overlapping with the peaks observed in VG30.

The obtained FTIR spectrums were also used to ascertain the chemical interaction between WMA additives and base asphalt binders. Figure 3.15 (c-j) indicates the spectral images of all the WMA binders along with the spectrum of their corresponding base asphalt binders (VG30 and PMB40). It was found that the characteristic spectral band of base asphalt binders and corresponding WMA binders were similar. Since neither a new peak nor the disappearance of existing absorbance peaks was observed, it can be stated that the addition of WMA additives, irrespective of their dosages, and base asphalt binders, resulted in physical interaction (no chemical reaction has

occurred). However, while comparing all the asphalt binders, a difference in the intensity of the absorbance peak was exhibited, depending on the base asphalt binders. Thus, the above interpretations confirmed that, though the interaction is purely physical, the type of base asphalt binder plays a vital role in manipulating the engineering properties of the WMA binders.

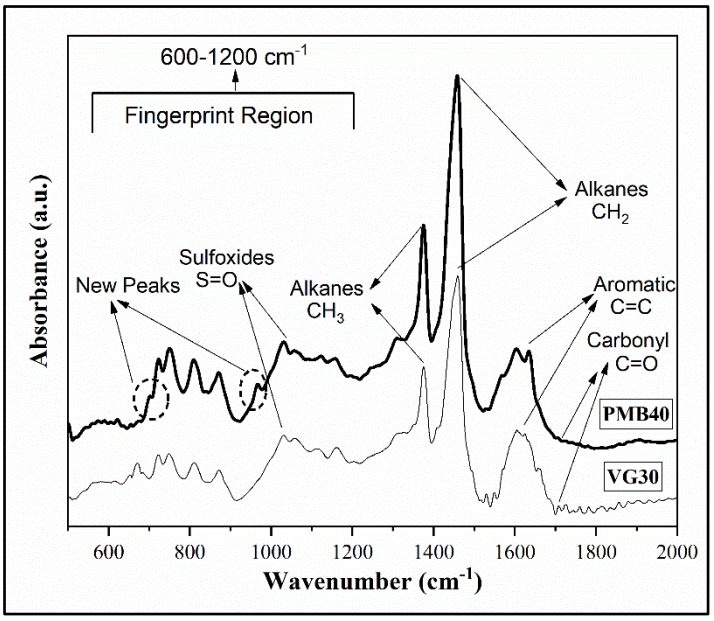

(a)

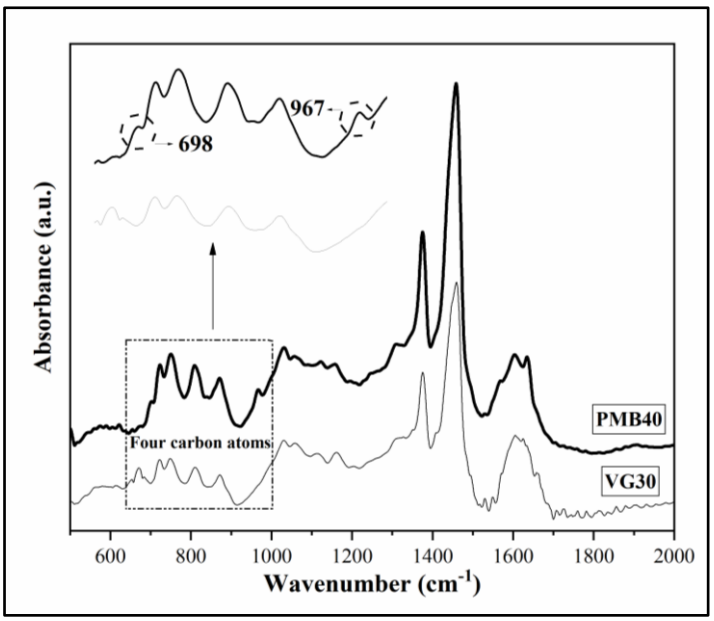

(b)

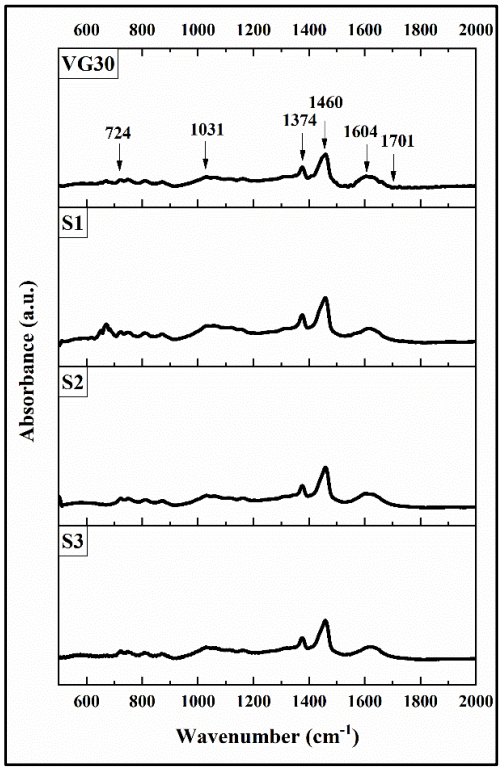
VG30
724
1031
1374
1460
1604
1701
S1
S2
S3
Absorbance (a.u.)
Wavenumber (cm-1)

(c)

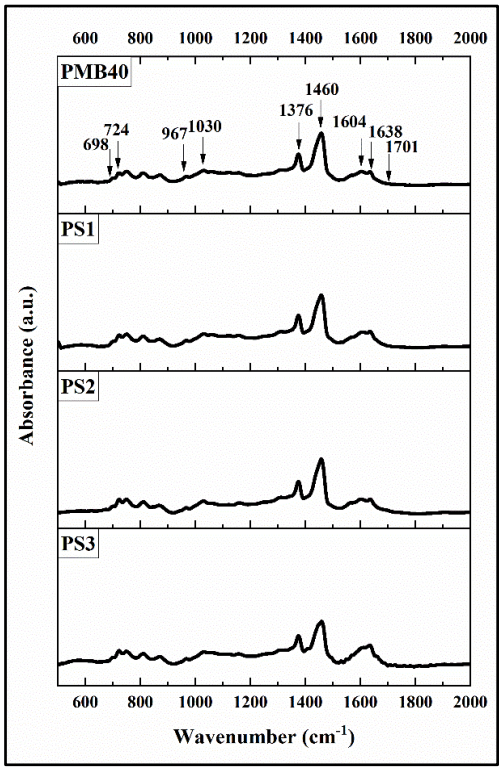
PMB40
698
724
967
1030
1376
1460
1604
1638
1701
PS1
PS2
PS3
Absorbance (a.u.)
Wavenumber (cm-1)

(d)

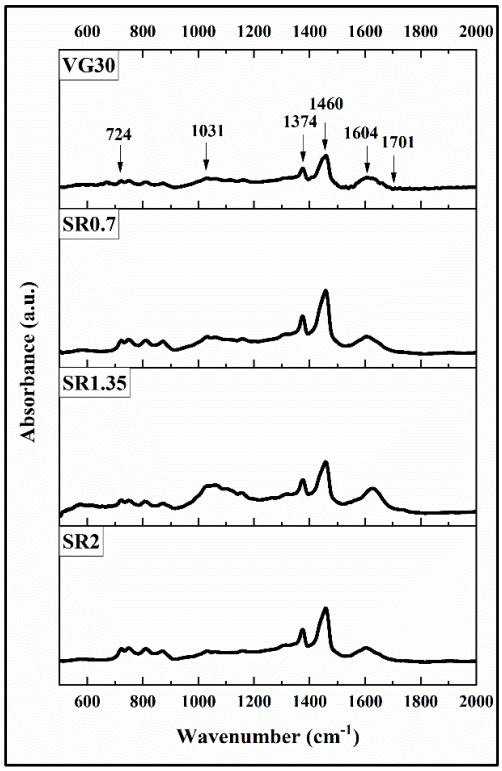
VG30
724
1031
1374
1460
1604
1701
SR0.7
SR1.35
SR2
Absorbance (a.u.)
Wavenumber (cm-1)

(e)

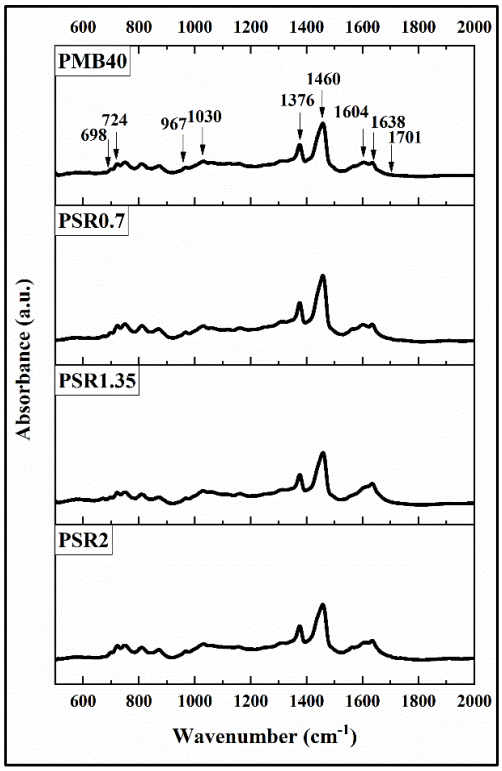
PMB40
698
724
967
1030
1376
1460
1604
1638
1701
PSR0.7
PSR1.35
PSR2
Absorbance (a.u.)
Wavenumber (cm-1)

(f)

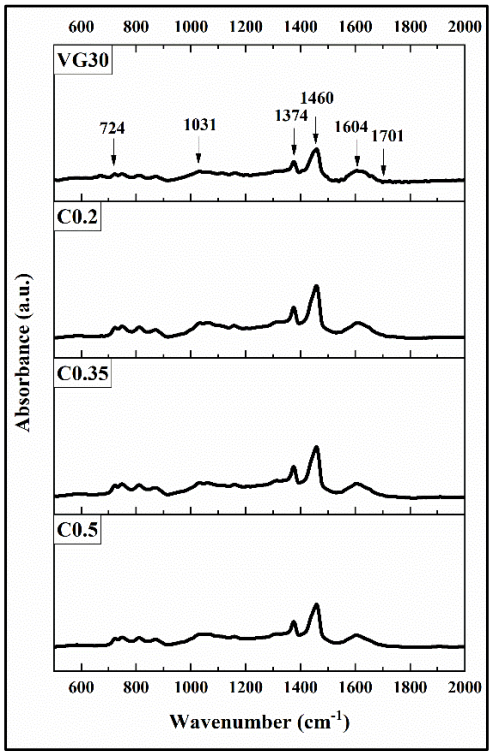

(g)

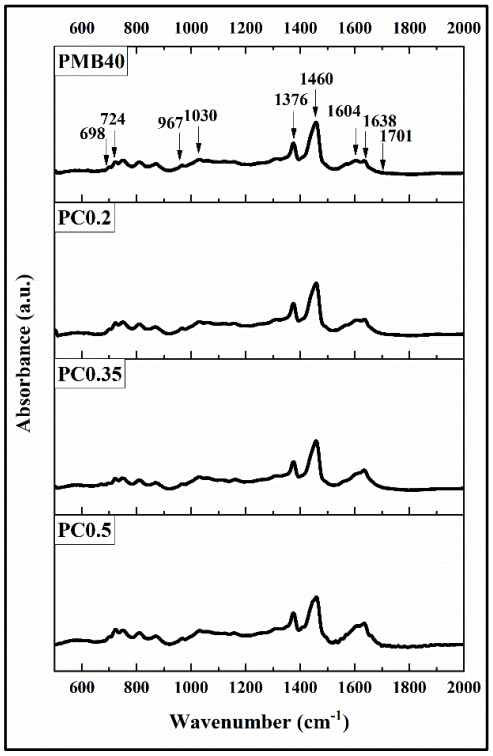

(h)

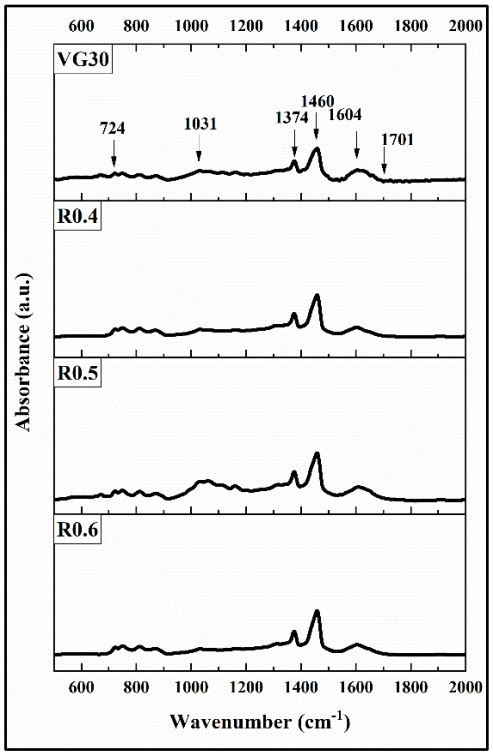

(i)

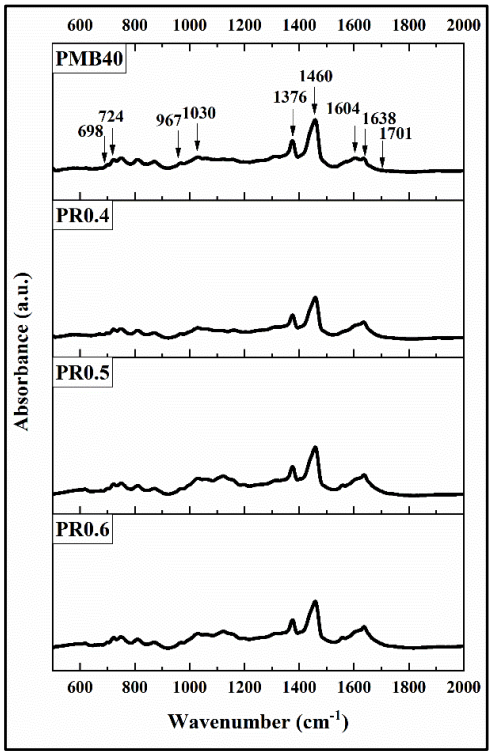

(j)

Figure 3.15. FTIR spectrums (a) Base asphalt binders, (b) Visualization of new peaks in PMB40, (c) S in VG30, (d) S in PMB40, (e) SR in VG30, (f) SR in PMB40, (g) C in VG30, (h) C in PMB40, (i) R in VG30, and (j) R in PMB40

3.4.1.3 Penetration Value

It is an empirical test that measures the consistency of the asphalt binder at 25 °C, wherein the penetration value is defined as the depth penetrated by a standard needle into a sample of asphalt binder in one-tenths of millimeters, under a load of 100 grams for 5 seconds. The test was done as per IS 1203 [453], and the test setup is shown in Figure 3.16a.

3.4.1.4 Softening Point

Softening point test determines the consistency of the asphalt binder using a ring and ball setup (Figure 3.16b). The temperature at which a standard steel ball, when placed over a brass ring containing the asphalt sample suspended in a water bath, starts flowing and travels a distance of 2.5 cm, when the temperature of the bath is increased at the rate of 5 °C per minute, is denoted as the softening point of the binder. Specifications as per IS 1205 [457] were used to conduct the test on different asphalt binder blends.

3.4.1.5 Viscosity Value

Absolute viscosity at 60 °C is generally used for the characterization of stiffness of asphalt binder at the average maximum temperature of the in-service pavement. A Cannon Manning viscometer (Figure 3.16c) was used to measure the absolute viscosity of all the blends used in this study. The time required for the asphalt binder to cross predefined timing marks within a viscometer tube under standard temperature and applied pressure, is used to calculate the viscosity of the binder. IS 1206 [454] was followed for the measurement.

(a) (b) (c)

Figure 3.16. Test setup (a) Penetration, (b) Softening point, and (c) Viscosity

3.4.1.6 High-Temperature Performance Grade (PG)

The conventional tests such as penetration and softening point are empirical and hence inadequate to fully characterize the viscoelastic behaviour of asphalt binders. Though viscosity measurements are fundamental, but, in general, fails to provide the information on the time dependency of asphalt binders. This led to the development of performance grade (PG) specifications, which characterizes the asphalt binders according to the climatic conditions under which it has to be used. PG is reported using two numbers. The first number is the average seven-day maximum pavement temperature, whereas the second number is the expected minimum pavement temperature. For example, PG 64-28 indicates that the asphalt binder with this grade can be used where the average seven-day maximum pavement temperature is 64°C, and the minimum pavement temperature likely to be experienced is -28°C. In the present research work, only the high-temperature PG was evaluated.

Anton Paar (SmartPave) MCR 102 DSR, as shown in Figure 3.17a, was used to measure high-temperature PG, using a parallel plate geometry initialized with a 25 mm diameter

spindle (Figure 3.17b) and 1 mm gap width. AASHTO M320 [488] was followed to obtain the high-temperature PG of all the prepared asphalt binders. In general, high-temperature PG is the maximum temperature at which the $|G^*|/\sin\delta$ in unaged conditions is more than 1 kPa. G^* indicates the complex modulus and is defined as the ratio of maximum applied shear stress to the maximum value of the resulting strain. On the other hand, δ represents the phase lag between the shear stress and shear strain response of the asphalt binder when subjected to an oscillatory test in DSR. The value of the PG temperature is usually checked at a difference of 6 °C. In addition to the high-temperature PG, the true fail temperature (the actual temperature beyond which the asphalt binders fail to meet the desired criteria) was also evaluated.

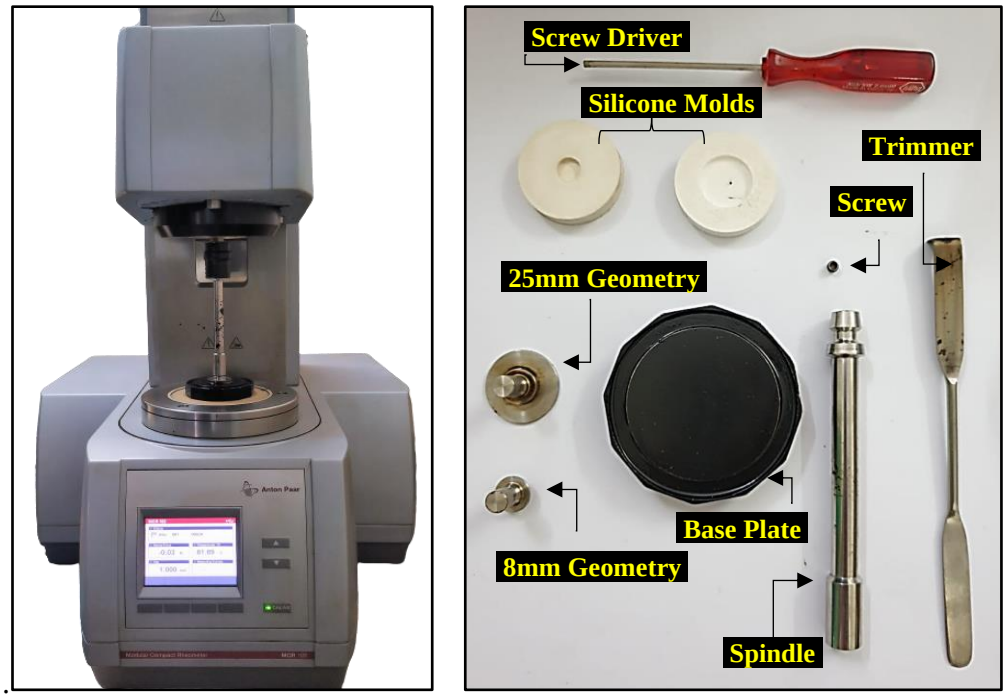

(a) (b)

Figure 3.17. (a) Dynamic shear rheometer (Anton Paar) MCR 102 and (b) DSR components and accessories

3.4.1.7 Discussion on the Basic Properties of Asphalt Binders

A series of basic properties, such as penetration, softening point, viscosity, PG, and corresponding fail temperatures, were evaluated to ascertain the physical behavior of asphalt binders. Figure 3.18 to Figure 3.21 indicate the effect of WMA additives and their dosages on the basic properties of VG30 and PMB40. It can be seen that the extent of change in the properties, with the addition of WMA additives, was different in both VG30 and PMB40. This variation is attributed to the difference in the interaction of WMA additives with the base asphalt binders, as also observed in SEM images. In addition, the change in the physical behavior of base asphalt binders, irrespective of their type, was found to be a function of WMA technology and their respective dosages. A detailed discussion on the influence of WMA additives is described in the next section.

3.4.1.7.1 Effect of WMA Technologies on the Penetration Value

Figure 3.18a and Figure 3.18b presents the penetration test results for different WMA binders prepared with VG30 and PMB40, respectively. It was found that the addition of Sasobit, irrespective of the base asphalt binder, considerably decreases the penetration value. In particular, the decrease in penetration value of VG30 and PMB40 was around 27-50% and 16-37%, respectively. This is attributed to the formation of crystalline lattice structure of waxy particles in Sasobit, which increases the stiffness and results in a lower penetration value. The extent of reduction was found to be dependent on its dosage. On the other hand, irrespective of the base asphalt binders, no noticeable difference in the penetration value was observed with the incorporation of other WMA additives (i.e., Sasobit Redux, Cecabase, and Rediset). The percentage in penetration was less than 10% relative to VG30 and PMB40. Interestingly, the effect of WMA additives was more prominent for VG30 than PMB40. This could be

associated with the dominance of crosslinking polymeric network in PMB40, as discussed in the previous section (SEM observations).

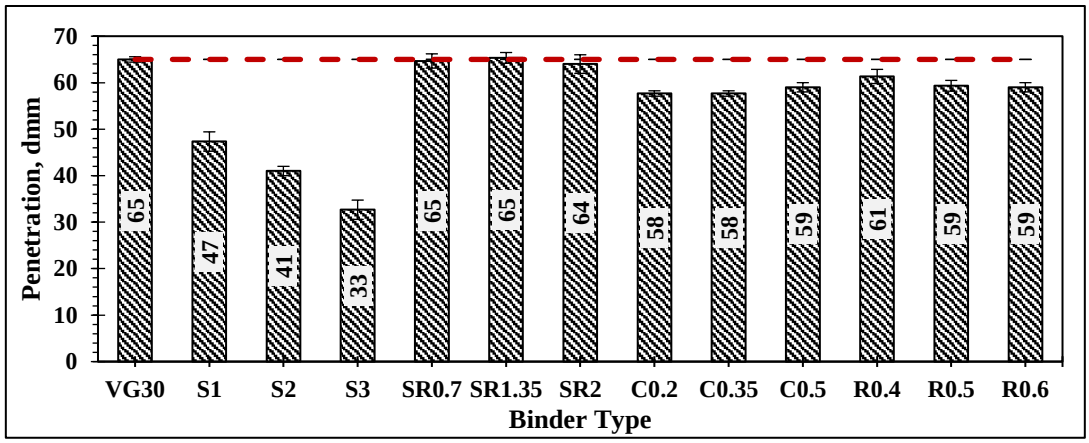

(a)

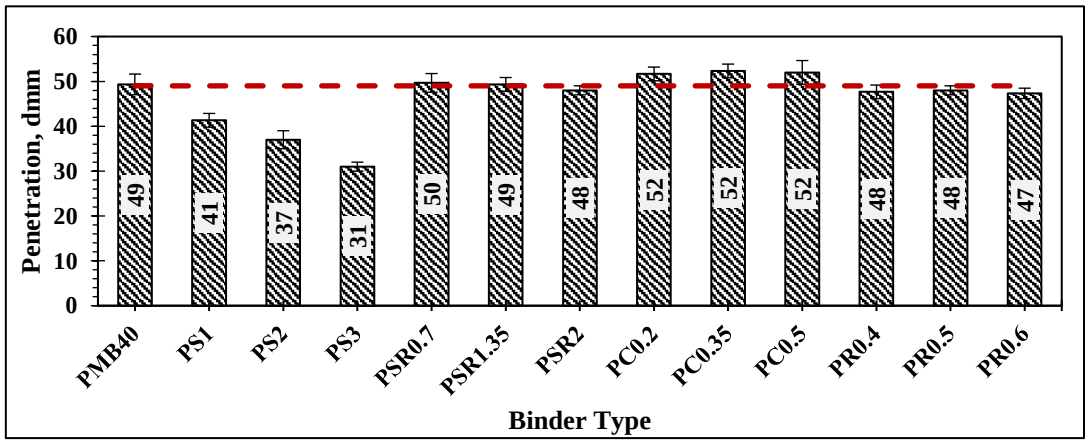

(b)

Figure 3.18. Penetration value of different WMA binders (a) VG30 base asphalt binder, and (b) PMB40 base asphalt binder

3.4.1.7.2 Effect of WMA Technologies on the Softening Point

Figure 3.19a and Figure 3.19b shows the variation in softening point of VG30 and PMB40, respectively, with the incorporation of WMA additives. Similar to the penetration value results, Sasobit-based WMA binders lead to increase in softening point for both the base asphalt binders (VG30 and PMB40). The shift in softening point

with the addition of Sasobit (irrespective of the dosage) was higher for VG30 (10-55%), as compared to PMB40 (3-13%). The change in softening point with the addition of other WMA additives (at any dosage) was found to be under 10% variability (as found in the penetration test results) compared to the softening point values of VG30 and PMB40.

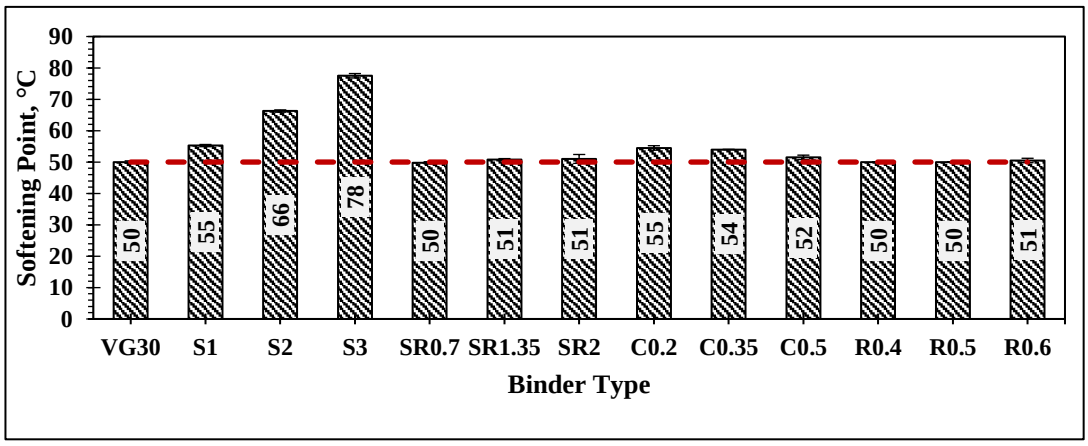

(a)

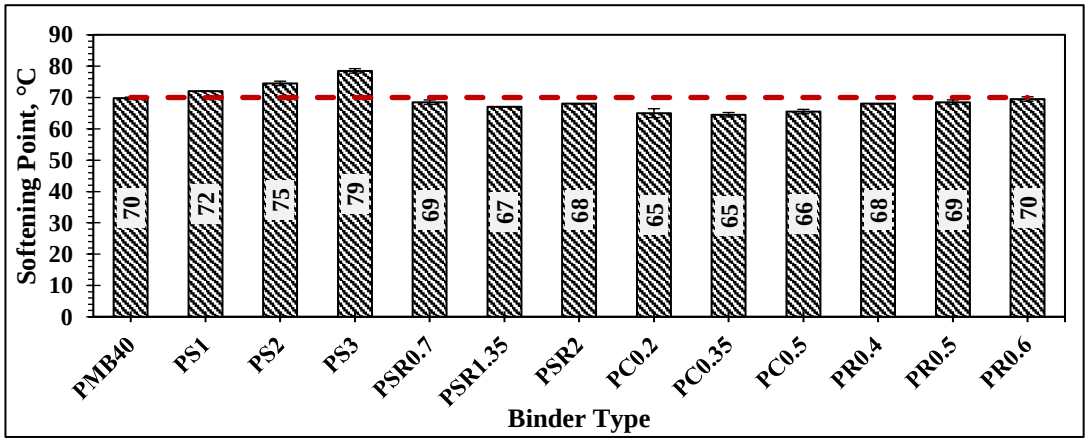

(b)

Figure 3.19. Softening point of different WMA binders (a) VG30 base asphalt binder, and (b) PMB40 base asphalt binder

3.4.1.7.3 Effect of WMA Technologies on the Viscosity Value

The effect of different WMA additives on the viscosity of VG30 and PMB40 are presented in Figure 3.20a and Figure 3.20b, respectively. It can be seen that the viscosity values of organic-based WMA binder, such as Sasobit, were higher than the viscosity of their respective base asphalt binders. Increase in dosage of the additive increased the viscosity value. The addition of 1%, 2% and 3% dosage of Sasobit shifted the viscosity value of VG30 from 280 Pa.s to 608, 1631, and 2337 Pa.s, respectively, indicating more than 100% increment at all the dosages. In the case of PMB40, around a 50% increment in viscosity value was found with PS1, while the percent change was over 100% (compared to PMB40), when PS2 and PS3 were tested. This is attributed to the crystallization effect of Sasobit at 60°C (viscosity test temperature), which might have increased the stiffness and so the resistance to flow (viscosity). It can be stated that Sasobit acts as a reinforcement agent to the asphalt binders as it restricts the flow behavior and increases the stiffness. Conversely, Sasobit Redux, being an organic-based WMA technology, did not indicate any variation in the viscosity of VG30 and PMB40. This is because the viscosity test was conducted at 60°C, which is around the congealing point of Sasobit Redux (where the wax terminates to flow), and hence it indicated similar characteristics as base asphalt binders.

The chemical-based WMA binder, such as Cecabase, did not indicate any remarkable change in the viscosity values of base asphalt binders. The obtained results were very similar to the respective viscosity of base asphalt binders (VG30 and PMB40). On the other hand, viscosity values of VG30 and PMB40 increased (around 3-25% for VG30 and 3-20% for PMB40) with the incorporation of Rediset. This behavior of Rediset was not observed in penetration and softening point tests, which are empirical in nature.

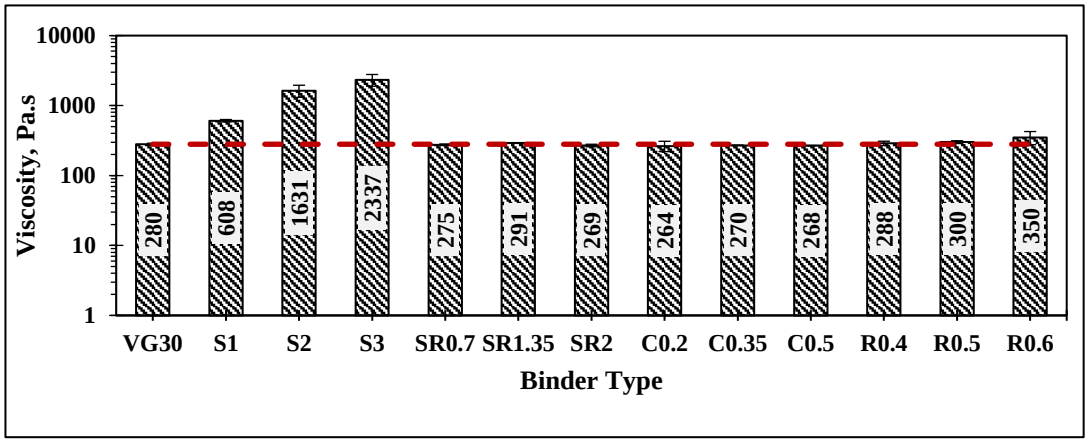

(a)

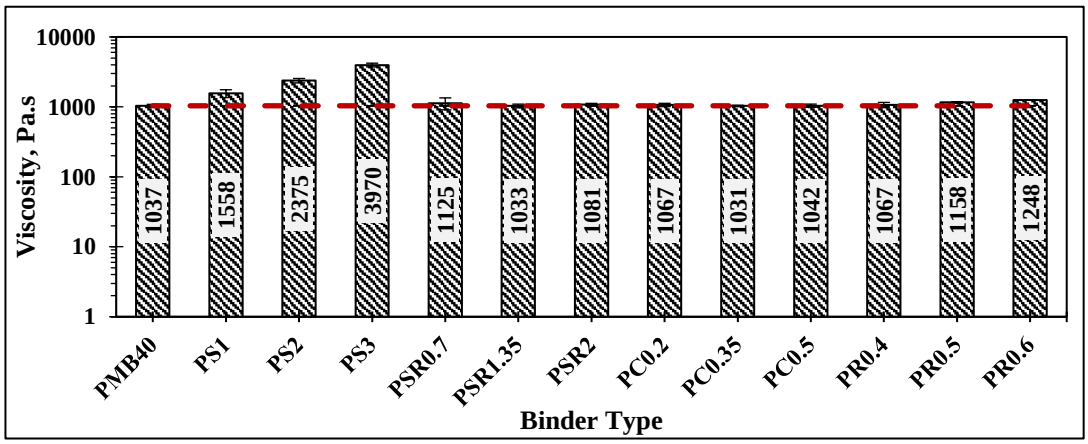

(b)

Figure 3.20. Viscosity values of different WMA binders (a) VG30 base asphalt binder, and (b) PMB40 base asphalt binder

3.4.1.7.4 Effect of WMA technologies on the high temperature PG

Asphalt binder is a viscoelastic material, which behaves like an elastic solid at lower temperature conditions, and viscous fluid at high temperature conditions. The basic characteristics of asphalt binder, such as penetration (empirical), softening point (empirical), and viscosity (though fundamental) vary considerably with the temperatures. Thus, these conventional tests fail to characterize the asphalt binders, especially when modified binders, such as PMB or WMA binders, are tested. PG, on the other hand, was developed as a fundamental rheological characterization method,

wherein the performance criteria is checked at expected high, intermediate and low temperatures. In this study, only the high-temperature PG was evaluated to compare VG30 and PMB40 with their corresponding WMA binders.

Figure 3.21 (a-b) shows the high-temperature PG obtained for different asphalt binders. In addition to PG, the true fail temperature is also presented. PG of VG30 was found to be lower than the PG of PMB40, and so does the true fail temperature. The PG and corresponding fail temperature of VG30 were found to be PG70 and 72.9°C, whereas PMB40 was characterized as PG82 grade asphalt binder, showing a fail temperature around 84.9°C. In VG30, the PG changed from PG70 to PG76 for S1 and PG82 for S2 and S3. Although S2 and S3 indicated similar PG, the true fail temperatures differed for both the WMA binders (i.e., 82.6°C for S2 and 84.7°C for S3). The improvement in PG and corresponding increment in true fail temperature reflects the increase in stiffness of VG30 with the increase in dosage of Sasobit. Since the interaction between VG30 and Sasobit additive was purely physical, as indicated in the FTIR spectrum (Figure 3.15c), the improvement in PG can be attributed to the crystallization of wax particles, as shown in SEM images (Figure 3.11 (a-c)).

In case of PMB40, the influence of Sasobit was found to be comparatively lower than VG30. The reason behind this aspect is that the PG of PMB40 was already near to the melting point of Sasobit wax, which retards the formation of crystalline lattice structure, and hence indicate similar PG for PS1 and PS2. Interestingly, as observed in the SEM image of PS3, the presence of few crystals leads to the shifting of PG to one grade higher from PG82 (for PMB40) to PG88 (for PS3). In addition, the true fail temperature for PS3 increased from 84.9°C (PMB40) to 89.3°C (PS3), indicating approximately 5% improvement.

Test results demonstrated that the addition of other WMA additives (Sasobit Redux, Cecabase, and Rediset), irrespective of base asphalt binders, neither affected the high-temperature PG nor the true fail temperature. Overall, all the WMA binders exhibited the same/improved PG, indicating similar/strong resistance against high temperature distresses, such as permanent deformation.

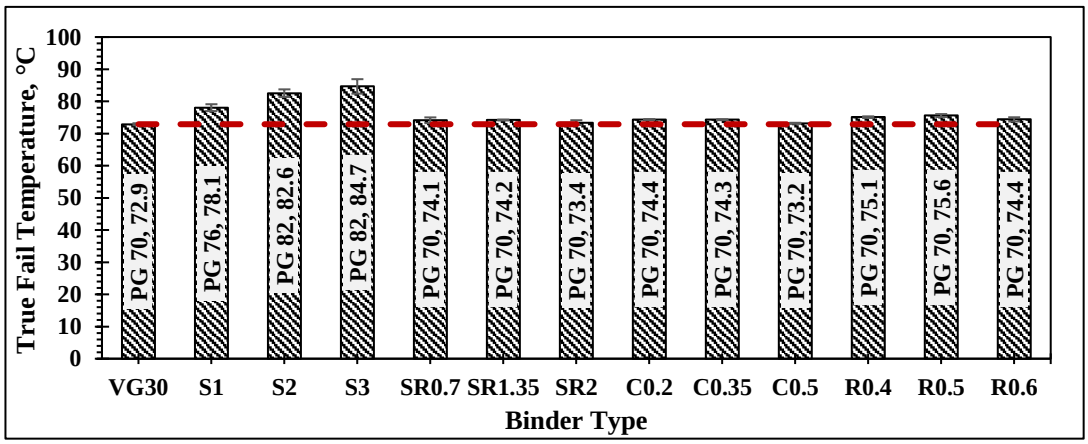

(a)

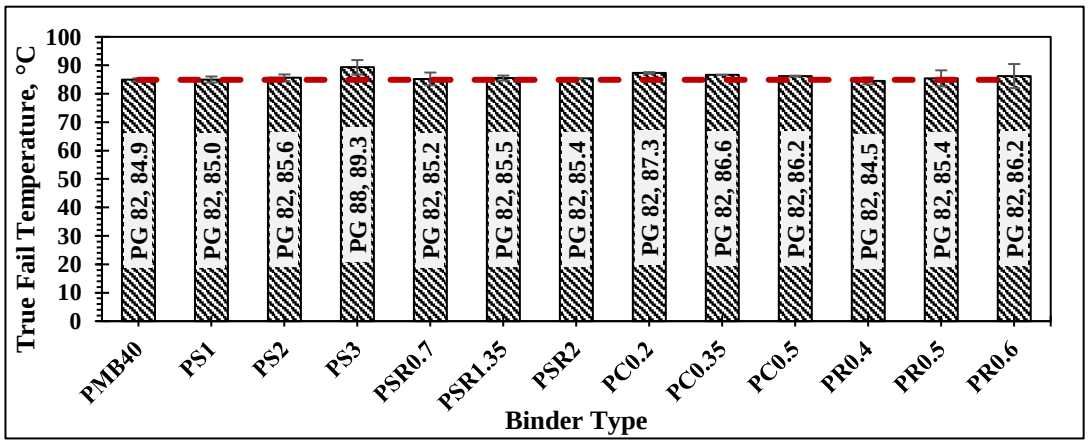

(b)

Figure 3.21. PG and True fail temperature of different WMA binders (a) VG30 base asphalt binder, and (b) PMB40 base asphalt binder

3.4.1.8 Correlations between the Basic Properties of Asphalt Binders

An attempt was made to identify the correlation between the basic properties of tested asphalt binders, irrespective of any test variables, such as binder type, WMA

technology, and additive dosage. Sometimes, the trend between the properties are useful to predict a given property of the binder using the results of another test method. The best-fit equation along with the corresponding coefficient of determination (R^2) value are shown in Figure 3.22 (a-f). In general, a higher softening point, viscosity, true fail temperature and a lower penetration are desirable for durable asphalt pavements. Strong inter-correlations were observed between the test parameters, except the correlation between true fail temperature and penetration (R^2=0.62), as shown in Figure 3.22c. The lower R^2 may be attributed to the difference in test mechanism, where penetration is an empirical test, and true fail temperature is a more fundamental rheological characterization method. Needless to say, the general trend between the above inter-correlated test parameters did not alter with the addition of WMA additives and change in base asphalt binders.

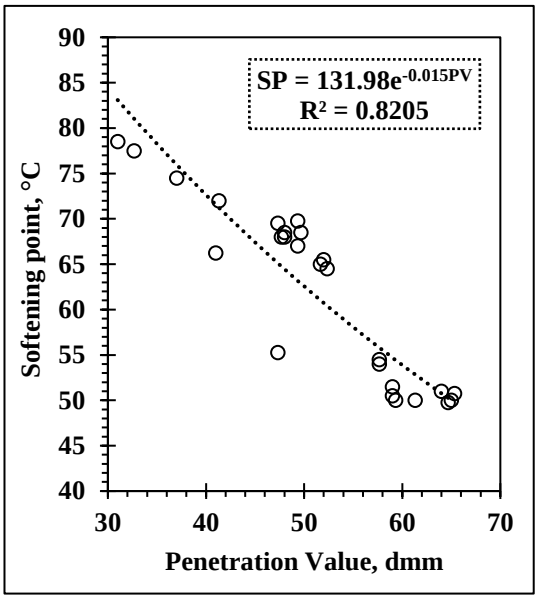

(a)

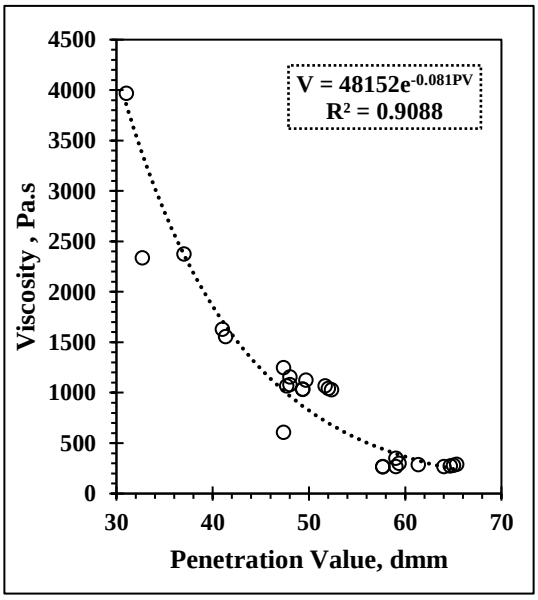

(b)

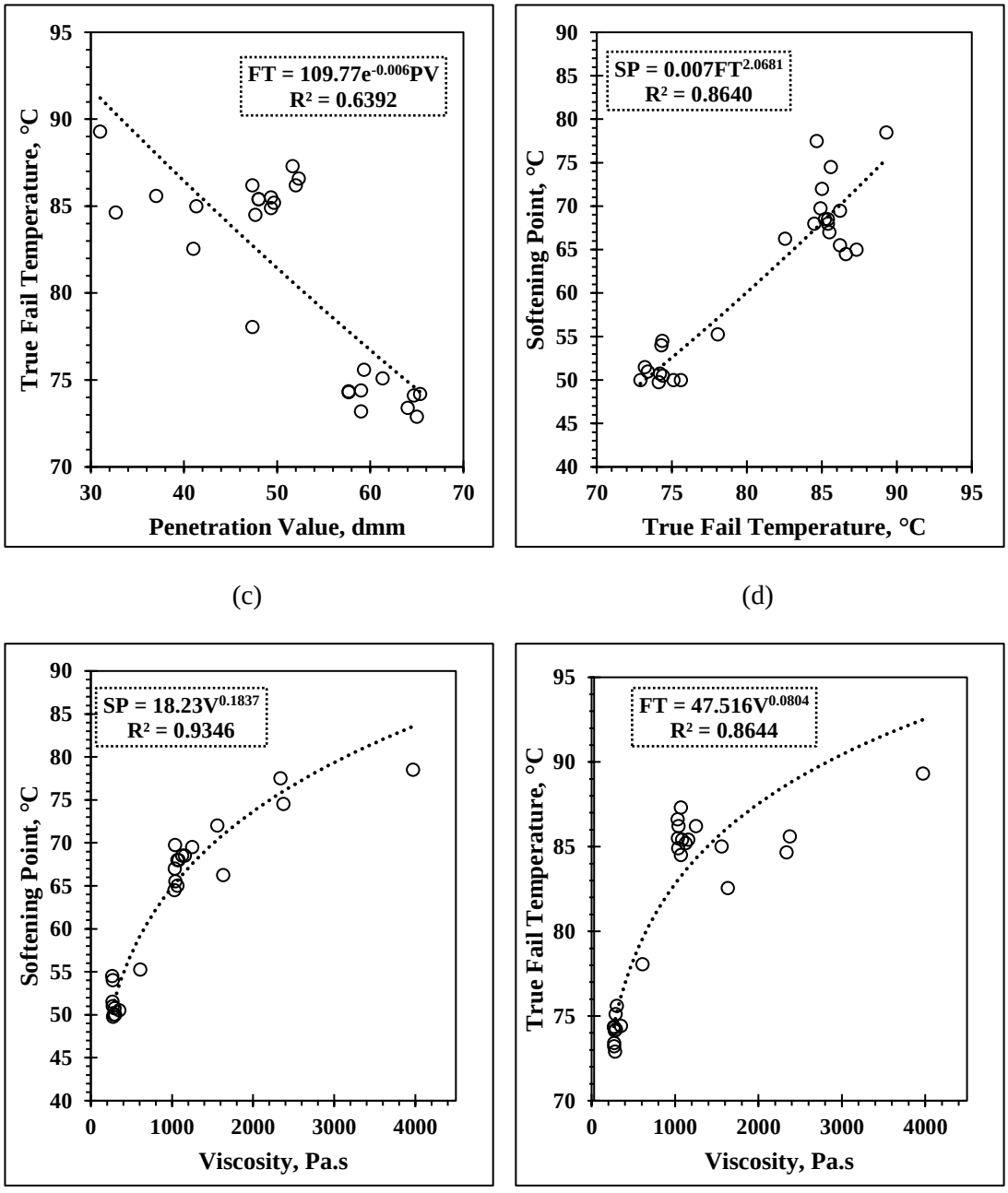

Figure 3.22. Correlations between different test parameters

Note: PV, SP, V and FT denote Penetration, Softening point, Viscosity, and True failure temperature, respectively.

3.4.2 Determination of Production Temperatures

Over a period of time, several methodologies have been proposed to determine the mixing and compaction temperatures of asphalt mixture. Though standard methods are available to determine the production temperatures of HMA, there are no standard methods to determine the mixing and compaction temperatures for WMA.

ASTM D2493 [131] provides guidelines for evaluating the production temperatures for HMA. The method is based on the viscosity of the asphalt binder, determined using a Rotational Viscometer (RV) (Figure 3.23). This method is popularly known as the equi-viscous (EQ) method [132]. As per the procedure, the temperature ranges, corresponding to the viscosity values of 0.17±0.02 Pa.s and 0.28±0.03 Pa.s, are taken as mixing and compaction temperatures, respectively, as shown in Figure 3.24. It is debated that the EQ method is not suitable for asphalt mixtures produced using modified binders, such as PMB and WMA binders [61,133,134]. Therefore, various alternative methods have been proposed and adopted for estimating the mixing and compaction temperatures of WMA mixtures. These methods, which are hypothesized to eliminate the limitations of the EQ method, require testing of asphalt binders using RV and/or DSR. Table 3.6 presents the formulation and limiting criteria of binder-based methods adopted in the present study to evaluate mixing and compaction temperatures. Different tests have different limiting criteria; for example, one test method recommends measuring the viscosity value corresponding to 0.001 s^{-1} while the other method commends 100000 s^{-1}. Since RV was conducted at a shear rate ranging from 10 s^{-1} to 100 s^{-1}, the viscosity value corresponding to other shear rates has to be predicted using some model techniques. One such model is the Carreau-Yasuda (C-Y) model (adopted in this study), which has been successfully applied to viscoelastic

materials, such as asphalt binders. The typical representation of measured data and C-Y fitting data is shown in Figure 3.25. Mathematically, the C-Y model is written as:

$$\frac{\eta - \eta_\infty}{\eta_0 - \eta_\infty} = [1 + (\lambda\dot{\gamma})^a]^{\left(\frac{n-1}{a}\right)} \quad (3.1)$$

Where η is the viscosity of asphalt binder, η_0 and η_∞ are zero and infinite shear viscosity, $\dot{\gamma}$ is the shear rate, λ, *n, and a* are the shape parameters, respectively.

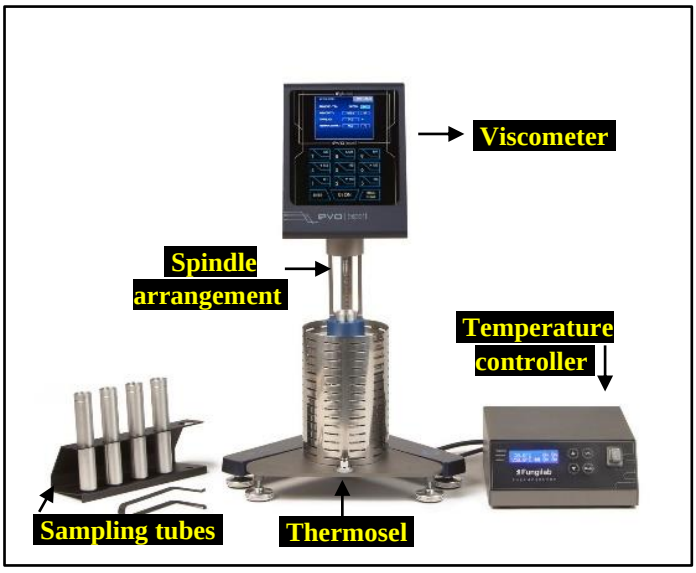

Figure 3.23. Rotational viscometer used in the present research work

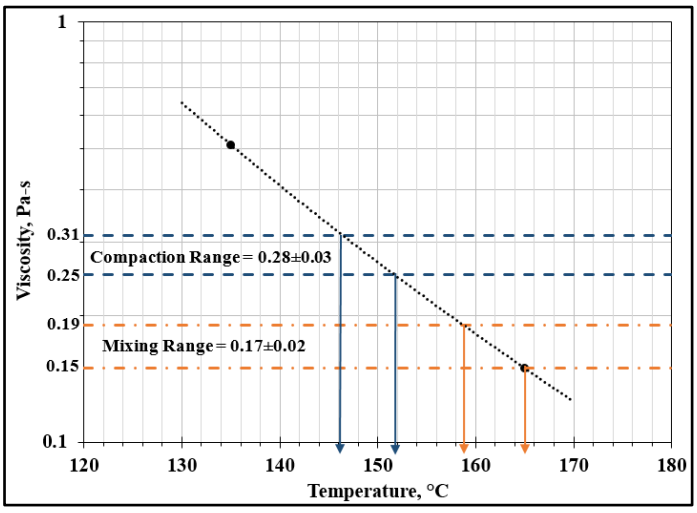

Figure 3.24. Viscosity-Temperature plot for determining mixing and compaction temperatures

Table 3.6. Representative list of proposed methods for the prediction of production temperatures

Method, Instrument, Reference	Viscosity Criteria	Shear Rate/Process	Temperatures
Equi-viscous (EQ) Method, RV, [131]	MT-0.17±0.02 Pa.s; CT-0.28±0.03 Pa.s	20 rpm	135˚C and 165˚C
Zero Shear Viscosity (ZSV) Approach, RV, [146]	MT-3.0 Pa.s; CT-6.0 Pa.s	0.001 s^{-1}	135˚C and 165˚C
Simplified ZSV Approach, RV, [139]	MT-0.75±0.05 Pa.s; CT-1.4±0.1 Pa.s	20 rpm	135˚C and 165˚C
High Shear Rate Method (HSR-O), RV, [147]	MT-0.17±0.02 Pa.s; CT-0.28±0.03 Pa.s	500 s^{-1}	135˚C and 165˚C
High Shear Rate Evolution Approach (HSR-E), RV, [135]	MT-0.275±0.03 Pa.s; CT-0.55±0.06 Pa.s	500 s^{-1}	135˚C and 165˚C
Flow Behavior Method, RV, [148]	MT-0.17±0.02 Pa.s; CT-0.28±0.03 Pa.s	100000 s^{-1}	135˚C and 165˚C
Phase Angle Method, DSR, [139]	MT- 325 $(\omega)^{-0.0135}$; CT- 300 $(\omega)^{-0.012}$	• Construction of master curve at 80 °C • Frequency corresponding to Phase angle of 86°	50°C, 60°C, 70°C and 80°C

Note: MT and CT indicate Mixing and compaction temperatures, respectively.

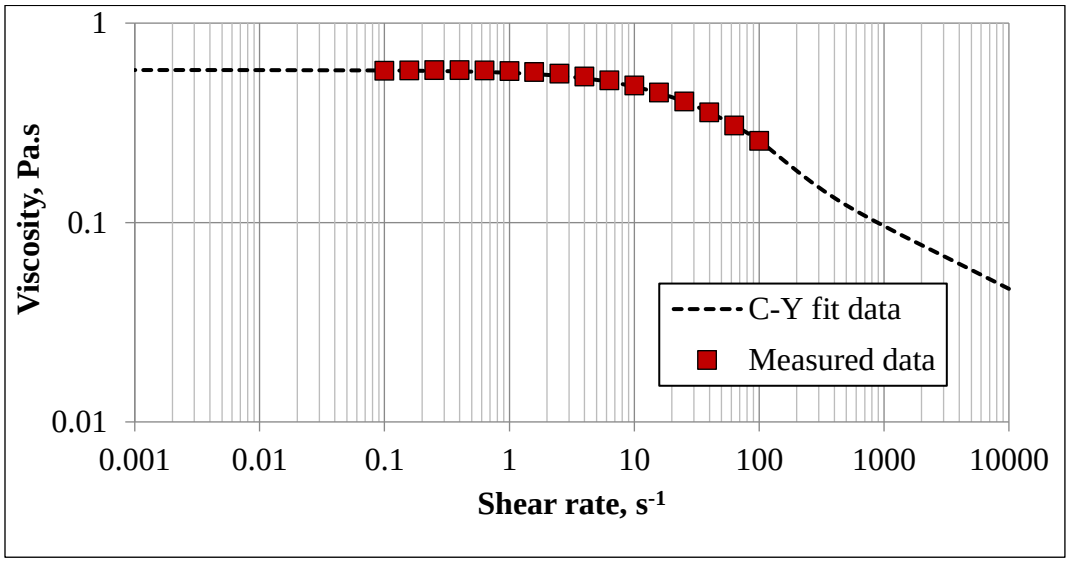

Figure 3.25. Typical representation of C-Y model curve

There has been a continuous debate on the reliability of viscosity-based methods. For WMA, viscosity-based methods may be applicable to the technologies that change the binder's viscosity [140]. However, WMA mixtures produced by foaming and chemical-based technologies have less influence on the viscosity of asphalt binder [92,130]. Thus, the production temperatures evaluated using conventional approaches may be unrealistic or inappropriate.

Past studies [219,220,489] have shown that the mechanism by which WMA technologies reduce the production temperatures could be related to the reduction in friction at the contact zone of the mineral aggregates and asphalt binder. This reduction in friction leads to improved workability in the asphalt mixture [490]. Thus, a workability-based method was proposed in this present study to rationally estimate the mixing and compaction temperatures of WMA mixtures. A workability apparatus, as shown in Figure 3.26, was fabricated, and its applicability was demonstrated by testing HMA and WMA mixtures. A new procedure, based on workability, was proposed and validated for rational evaluation of production temperatures. The reduction in mixing

and compaction temperatures obtained for different WMA technologies were also compared.

A two-step validation process was adopted in this study. First, the obtained mixing temperatures were validated using a novel coating ability test. A simple experimental setup was fabricated to quantify the coating of asphalt binder through an image analysis procedure. The line diagram of the developed setup is shown in Figure 3.27a. At the mixing temperature, it is expected that the asphalt binder will sufficiently coat the aggregate particles (Figure 3.27b). Secondly, for the validation of compaction temperature, air voids of compacted mixtures (Figure 3.27c), obtained using an impact compactor (Figure 3.27d), were evaluated. This was done to ensure that at the compaction temperature appropriate density in the asphalt mixtures is obtained. For both the validation, samples prepared using VG 30 and PMB 40 were taken as the reference for their respective WMA samples. The details of the working principle, the procedure for finding the production temperatures, and their validations are discussed in chapter 4.

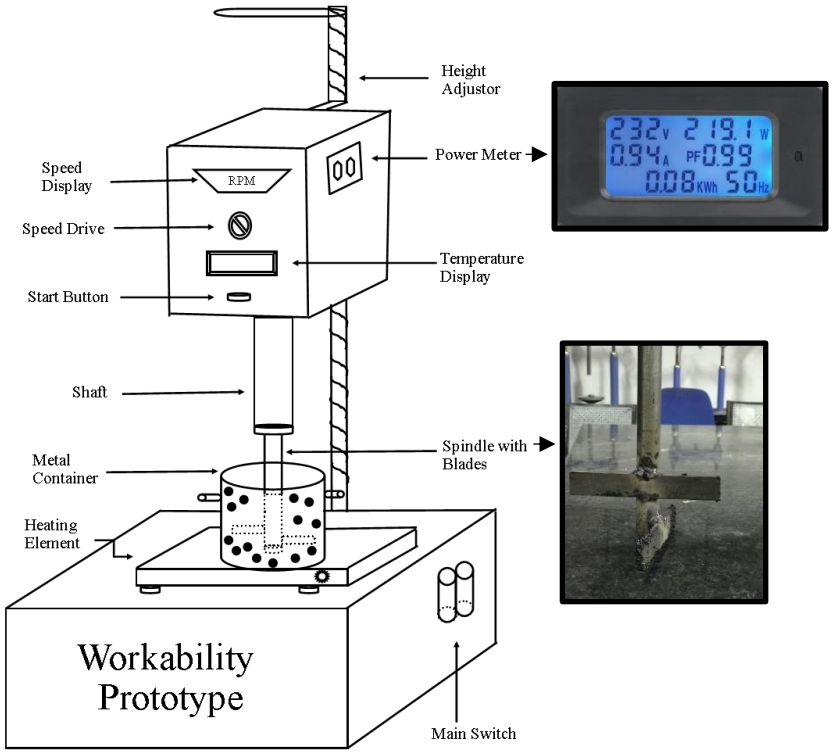

Figure 3.26. Line diagram of developed workability prototype

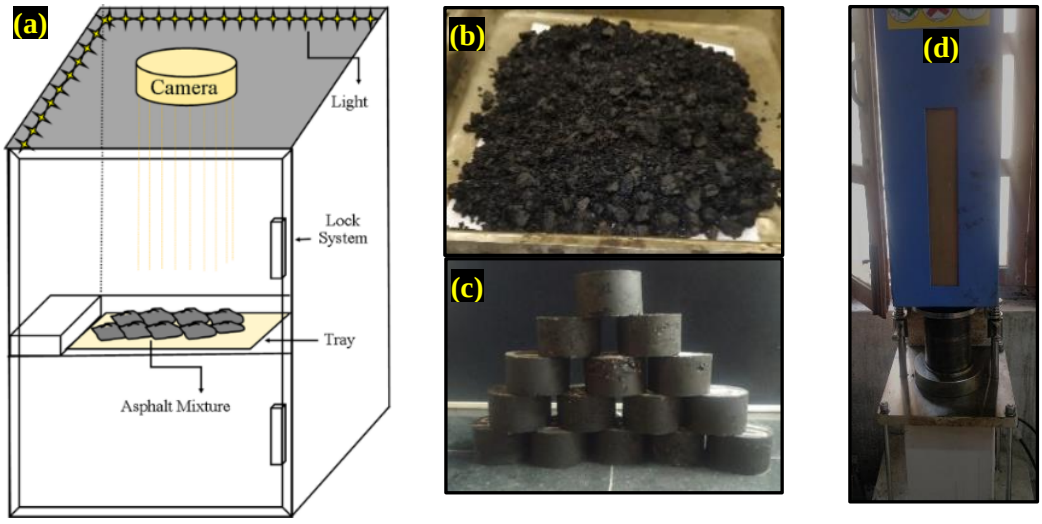

Figure 3.27. Validation checks (a) Coating setup, (b) loose asphalt mixture for coating, (c) compacted asphalt mixtures, and (d) Impact compactor

3.4.3 Phase I – Characterization of Asphalt Binders

3.4.3.1 Frequency Sweep

Frequency sweep (FS) test (using a DSR) on asphalt binders was performed over a range of frequencies (0.1-100 rad/sec) at different temperatures (10 °C to 70 °C). 8 mm diameter spindle (Figure 3.17b) with 2 mm plate gap was used for 10-30°C, whereas 25 mm spindle (Figure 3.17b) with 1 mm plate gap was used for 40-70°C, with parallel plate geometry. The test was conducted under the linear viscoelastic (LVE) regime of the asphalt binders at all the test temperatures. Time-temperature superposition principle (TTSP) is a competent tool for describing the viscoelastic behavior of linear polymers over a broad range of time and frequency, by shifting data obtained at several temperatures to a common reference temperature [491,492]. By obtaining data at several temperatures for a measurable range of frequency, a master curve could be plotted at a single reference temperature which could cover many decades of frequency/time (as shown in Figure 3.28). The data from the FS test was used to construct $G^*/\sin\delta$ and $G^*.\sin\delta$ master curves at reference temperatures of 60 °C and 20 °C, respectively. The choice of reference temperatures was based on the average maximum and average minimum temperatures commonly found in tropical climates. $G^*/\sin\delta$ has been correlated with rutting, while $G^*.\sin\delta$ has been used to explain the fatigue behavior of asphalt binders under the LVE range.

Previous literatures [493–495] revealed that AASHTO M320 and AASHTO T315 failed to capture the performance of some modified asphalt binders. In this direction, accelerated rutting and fatigue tests such as multiple stress creep and recovery (MSCR) and linear amplitude sweep test (LAST), respectively, have been developed. These accelerated tests have been discussed in the subsequent sections.

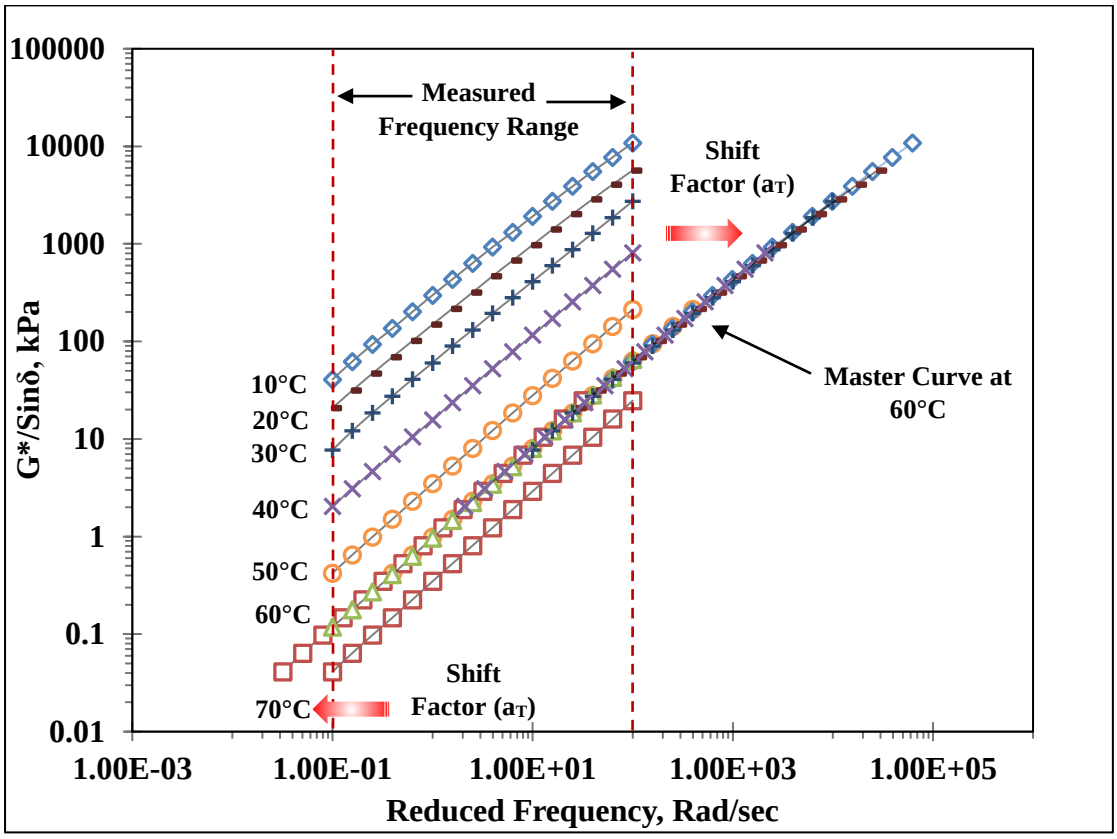

Figure 3.28. Example of master curve (G*/Sinδ) at reference temperature of 60°C

3.4.3.2 Multiple Stress Creep and Recovery (MSCR)

MSCR test [496] is one of the popular test methods used to evaluate the rutting resistance of asphalt binders. Previous studies [497–499] have shown a good correlation between the results of MSCR test and rut depth of asphalt mixtures. MSCR test was conducted on STA samples using a 25 mm spindle and a 1 mm gap setting in the DSR following AASHTO T 350 [496]. According to the specification, the binder is subjected to an alternate cycle of 1-second creep and 9-second recovery, at stress levels of 0.1 kPa and 3.2 kPa. This is a continuous test, where ten loading cycles are given at each stress level. In addition to 0.1 kPa and 3.2 kPa, two additional stress levels (5 kPa and 10 kPa) were also chosen in this study. This was done to assess the response of the binders when subjected to higher stress levels. Previous studies [468,500,501] have also

recommended using higher stress levels to assess the rutting resistance of asphalt binders through the MSCR test. In this study, four different test temperatures, i.e., 40 °C, 50 °C, 60 °C and 70 °C, were chosen to evaluate the rutting resistance of base asphalt binders and WMA binders. The choice of these temperatures is in agreement with previous studies [90,468,497]. The rutting susceptibility of the binders was evaluated by calculating the non-recoverable creep compliance (J_{nr}) and percent recovery (%R) from the measured data. J_{nr} is the ratio of unrecoverable strain to the applied stress, while %R is the percentage of recovered strain. Both J_{nr} and %R values are averaged over all the cycles at a particular stress level. A typical schematic response obtained in the MSCR test along with the calculation of J_{nr} and %R is presented in Figure 3.29.

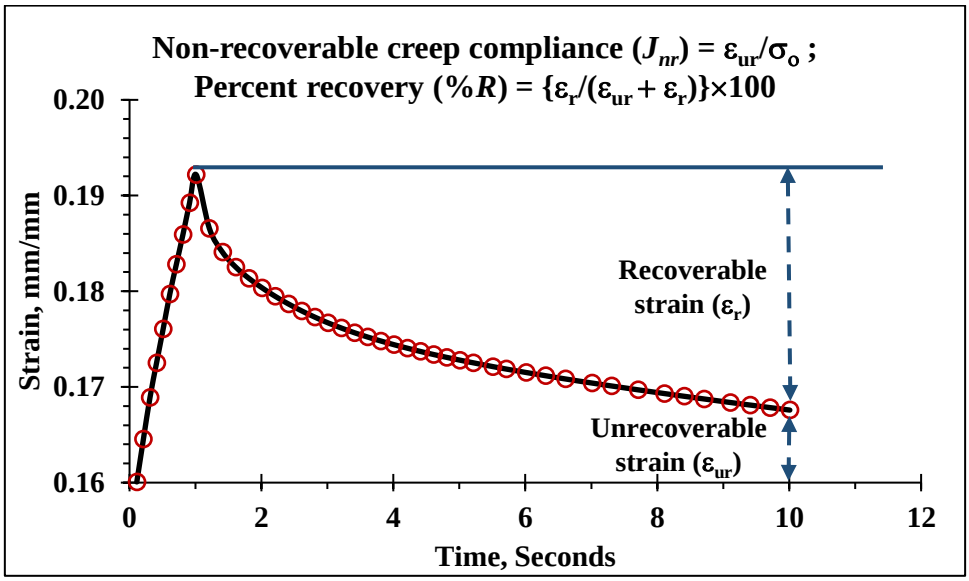

Figure 3.29. Schematic representation of creep and recovery

3.4.3.3 Linear Amplitude Sweep Test (LAST)

LAST is an accelerated test to evaluate the fatigue life of asphalt binders using DSR [477]. In this test method, the viscoelastic continuum damage (VECD) principle is used

to derive the damage characteristics of the binders when subjected to continuous increasing strain amplitude [502]. LTA samples were used in the LAST using an 8 mm diameter spindle and a 2 mm gap at temperatures of 10 °C, 20 °C and 30 °C. LAST was performed in accordance with AASHTO TP 101-14 [503] to determine the parameter *A* and *B*, required in the asphalt binder fatigue equation, which can be written as:

$$N_{\mathrm{F}} = A(\gamma_{\max})^{B} \tag{3.2}$$

This test, as per the standard procedure, was conducted using a two-step procedure. First, a frequency sweep test was done at a low stain amplitude of about 0.1% to obtain an undamaged material property, α, which is used to calculate the parameter *B* in the above equation (B= -2α). This was followed by an amplitude/strain sweep test conducted at a frequency of 10 Hz, with a linearly increasing load amplitude from 0.1% to 30% in 300 seconds. The amplitude was increased at a rate of 1%, subjecting the binder to 100 cycles at each strain value. This step was used as an input in viscoelastic continuum damage (VECD) analysis for the determination of *A*.

3.4.3.4 Bond Strength and Bond Strength Ratio

Pneumatic Adhesion Tensile Testing Instrument (PATTI) quantum gold was used to measure the pull-off strength/bond strength between the aggregate matrix and asphalt binder in accordance with AASHTO T361 [331]. Figure 3.30 shows the pneumatic piston setup used in the present study. Bond strength (BS) can be calculated using equation 3.3, as specified in AASHTO T361 [331].

$$BS = \frac{(BP \times A_g) - C}{A_{ps}} \tag{3.3}$$

Where BS and BP are bond strength (kPa) and burst pressure (kPa), respectively; A_g denotes the contact area of gasket combined with reaction plate (mm^2); A_{ps} refers to the area of pull stub (mm^2), and C is the value of piston constant.

In the present study, aggregate substrates (as shown in Figure 3.30) were prepared after cutting large size aggregates into small sizes. Following the cutting process, the surface of testing substrates was polished by applying extrafine #280 silicon carbide (SiC) grit (average size: 39-45 microns) to remove the cutting traces and ensure a consistent surface roughness. The grit number denotes the number of holes per square inch in the sieve from which the grains are passed. More the number of holes, finer will be the abrasive grains. These micro grits are too fine to cause any effect on the surface texture of the aggregates, rather it removes a tiny amount of material for maintaining uniform surface characteristics. Further, the surface of the aggregate substrates was cleaned and dried by subjecting them in a draft oven at a controlled temperature of 150°C for a minimum of 30 minutes as per AASHTO T361 [331]. Drying was done to remove any residual moisture entrapped within the aggregates. Next, the dried polished aggregates and the stub were heated at the obtained mixing temperature (which varies with the type of WMA additives and aggregate source). The asphalt binder, on the other hand, was heated to the respective mixing temperature and poured into a silicone mold (Figure 3.17b), which was further cooled. The asphalt binder was attached to the preheated stub and pressed against the aggregate (preheated) surface. The pull-off force required to detach the stub from the aggregate substrate was measured. Failure occurs when the applied force is higher than the adhesive/cohesive strength. The test was carried out on dry and moisture exposed specimens to study the moisture sensitivity using the BS approach. Moisture resistance was assessed in terms of bond strength ratio (BSR) (as shown in equation 3.4), which is the ratio of BS in wet (exposing the sample in moisture

for 24 hours at 40°C) and dry conditions. A higher BSR value represents better resistance against moisture-induced damage. Figure 3.31 shows the stepwise procedure adopted in the present study for the evaluation of BS and BSR.

$$BSR = \frac{BS_{Wet}}{BS_{Dry}} \tag{3.4}$$

Where BSR is bond strength ratio in %; BS_{Wet} and BS_{Dry} are the bond strength in wet and dry conditions, respectively.

Figure 3.30. Pneumatic piston setup with different testing components

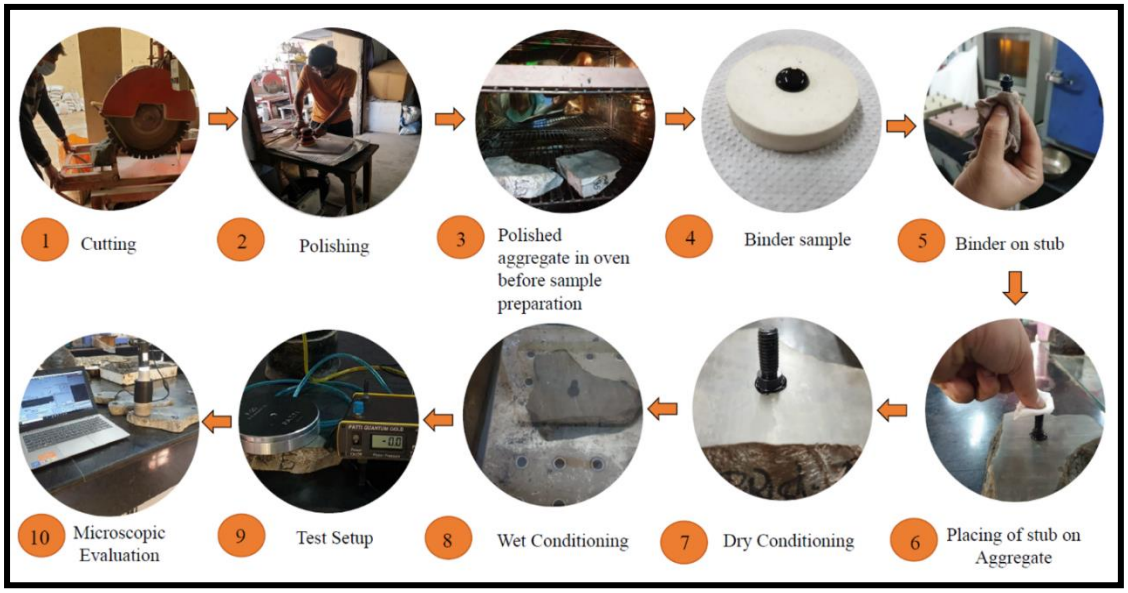

Figure 3.31. Stepwise procedure to determine BS and BSR

3.4.4 Phase II – Characterization of Asphalt Mixtures

3.4.4.1 Mix Design

Bituminous Concrete (BC) (Grading II) with a nominal maximum aggregate size (NMAS) of 13.2 mm was designed as per the specifications of the Ministry of Road Transport and Highways (MoRTH), India [1]. Figure 3.32 shows the obtained gradation for both the aggregate types (granite and dolomite) and specification limits for BC (grading II). Marshall mix design, as per Asphalt Institute specification (MS-2) [136], was used to prepare asphalt mixtures. At first, trial mixes were prepared at different binder content (5%-7%) and the optimum binder content (OBC), corresponding at 4% air voids, was evaluated for samples prepared using VG30 and PMB40.

In general, the construction and laying of WMA mixtures are similar to HMA mixtures [21,92]. Wang et al. [75] indicated that the mix design protocols of WMA mixtures are similar to conventional HMA mixtures. As per the preliminary investigations carried out in the laboratory using randomly selected WMA additives and aggregate sources, the OBC for WMA mixtures were found to be same as HMA. This observation has been confirmed by various literatures [77,173,504], where it was reported that WMA has a minor influence on the OBC and volumetric characteristics of asphalt mixtures. Since the present study aimed to evaluate the influence of different WMA additives on the production temperatures and performance of asphalt binders and mixtures, the obtained OBC (for HMA) was used to prepare WMA mixtures. All the test parameters, except the mixing and compaction temperatures, were kept constant throughout the study for analyzing HMA and WMA mixtures. The mixing and compaction temperatures required for the preparation of WMA mixtures were obtained based on

the workability test, as explained in the Chapter 4. The mix design results of BC (grading II) with VG30 and PMB40 are presented in Table 3.7.

In general, asphalt mixtures should be produced to perform satisfactorily after construction. This can be ensured by production of asphalt mixtures that are resistant to rutting, fatigue cracking and moisture-related distresses (Figure 3.33 (a-c)). Simple mix design parameters such as volumetric properties, Marshall stability, and flow value cannot be used for assessing the performance of asphalt mixtures. Thus, the asphalt mixtures (HMA and WMA) prepared at the OBC were judged based on different performance-based test methods such as the Cyclic compression test (CCT) for rutting and Indirect tensile cracking test (Ideal CT) for fatigue cracking. A check against moisture damage was also ascertained by carrying out a Boiling water test, retained Marshall stability (RMS), and modified Lottman test. The asphalt mixtures were tested in UA, STA, and LTA conditions based on the specified requirement of the test method.

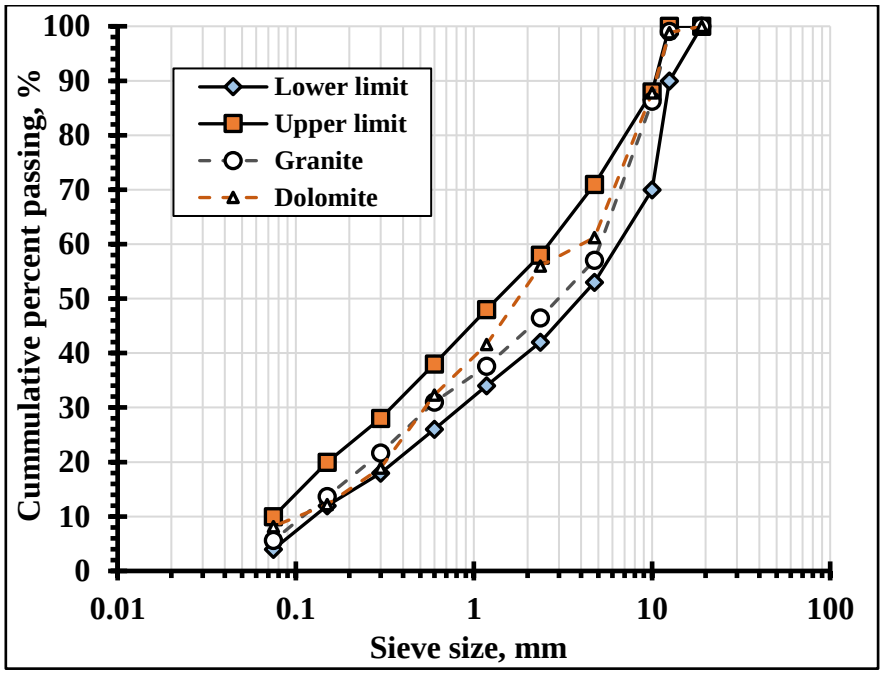

Figure 3.32. Designed aggregate gradation for both the aggregate source

Table 3.7. Mix design attributes of conventional HMA mixtures

Binder Type	**VG30**		**PMB40**		**Specification Limits** [505]
Aggregate Type	**Granite**	**Dolomite**	**Granite**	**Dolomite**	
OBC, %	5.8	5.6	6	5.9	Min. 5.4
G_{mb}	2.407	2.408	2.357	2.403	-
G_{mm}	2.509	2.506	2.460	2.507	-
Air voids, %	4.07	3.91	4.19	4.13	3-5
VMA, %	14.05	13.83	15.58	14.27	Min. 12
VFB, %	71.07	71.73	73.13	71.05	65-75
Stability, kN	14.86	14.42	17.76	17.49	>9
Flow, mm	3.60	4.13	4.15	3.76	2-4

Note: OBC, G_{mb}, G_{mm}, VMA, and VFB refer to optimum binder content, bulk specific gravity of the mix, theoretical specific gravity of the mix, voids in mineral aggregates, and voids filled with bitumen, respectively.

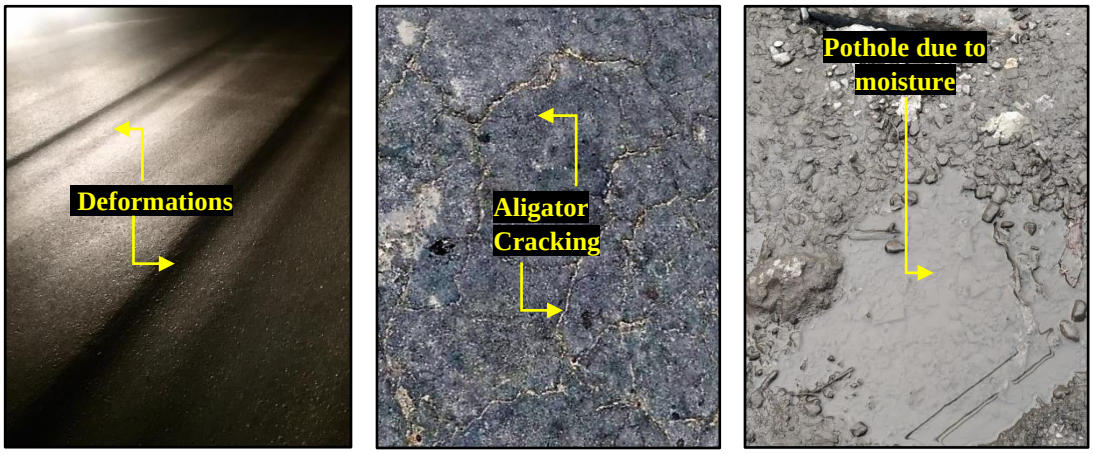

(a) (b) (c)

Figure 3.33. Form of distresses (a) Rutting, (b) Fatigue, and (c) Moisture

3.4.4.2 Cyclic Compression Test (CCT)

CCT was conducted to compare the rutting potential of HMA and WMA mixtures prepared using VG30 and PMB40. The testing was conducted on STA asphalt mixtures using a dynamic testing system (DTS), DTS-30, at a controlled temperature of 60°C. The compacted samples (having 7% air voids) were conditioned at the testing temperature for 2 hours prior to testing. Immediately after the conditioning, the test sample was placed at the center coaxially with the loading axis between the two platens, as shown in Figure 3.34a. Initially, a preload of 10±2 kPa was applied for 10 minutes as specified in EN12697-25 [506]. Thereafter, the specimen was subjected to a cyclic axial pulse loading with a frequency of 0.5 Hz and a load of 100±2 kPa. Periodic load was applied with a loading time of 1 second followed by a rest period of 1 second in accordance with EN 12697-25 [506]. The test was terminated at 3600 cycles or 4% accumulated strain, whichever occurred earlier. Figure 3.34b shows the schematic representation of the CCT curve along with the indication of deformation at each stage. The curve generally comprises of 3 stages response, i.e., primary, secondary and tertiary. The primary stage shows the quick accumulation of permanent deformation; the secondary stage indicates the increase in accumulated strain with a constant slope, and the tertiary stage displays the regain in accumulative strain. There exist one more component of creep which is observed before the primary stage, i.e., Instantaneous strain. These strains arise due the adjustment of sample during initial cycles. Instantaneous strains are fully recoverable, meaning no permanent strain is initiated during the loading and rest period.

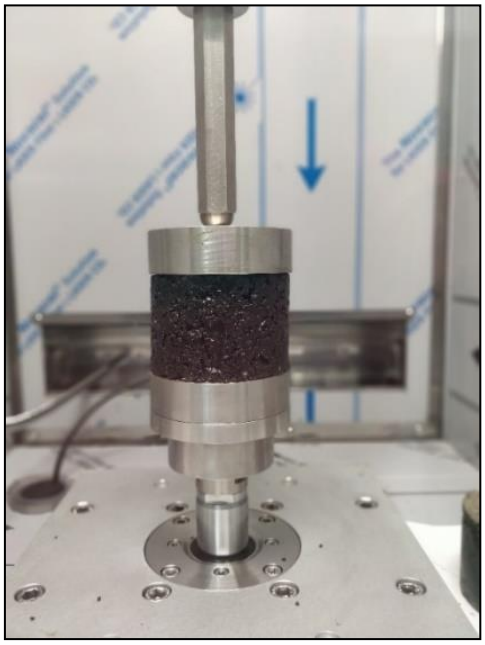

(a)

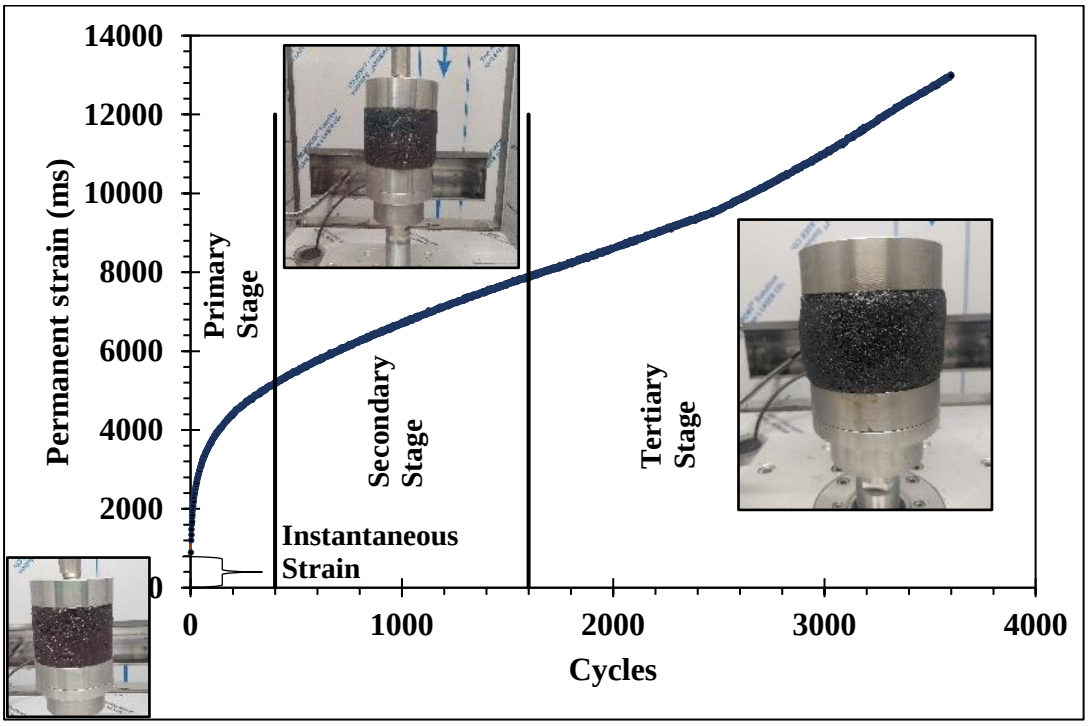

(b)

Figure 3.34. Cyclic compression test (a) Setup in DTS-30, and (b) Schematic representation of CCT curve

3.4.4.3 Indirect Tensile Cracking Test

Fatigue potential or cracking resistance of the HMA and WMA mixtures was evaluated using an indirect tensile cracking test. This test is popularly known as Ideal CT and can be performed using DTS-30. The test was conducted at 20°C following ASTM D8225 [507]. LTA conditioned specimens with a diameter of 101.6 mm, compacted at 7% air voids, were tested at a constant load-line displacement rate of 50 mm/minute. Figure 3.35a and Figure 3.35b show the test setup of Ideal CT and schematic load-displacement curve along with the indication of crack propagation on the surface of asphalt mixtures, respectively.

The load-deformation curves were recorded to determine the work of fracture (W_f), fracture energy (FE), and peak load (P_{Max}). W_f is the area under the load versus deformation curve, whereas the FE is defined as the failure energy required to induce a unit surface area of a crack and is calculated as the W_f divided by the diameter and the thickness of the specimen. In general, a higher value of FE indicates higher fatigue resistance.

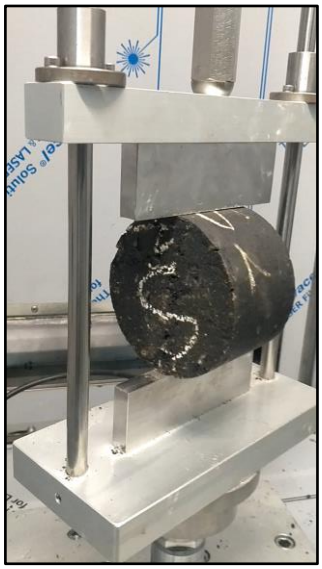

(a)

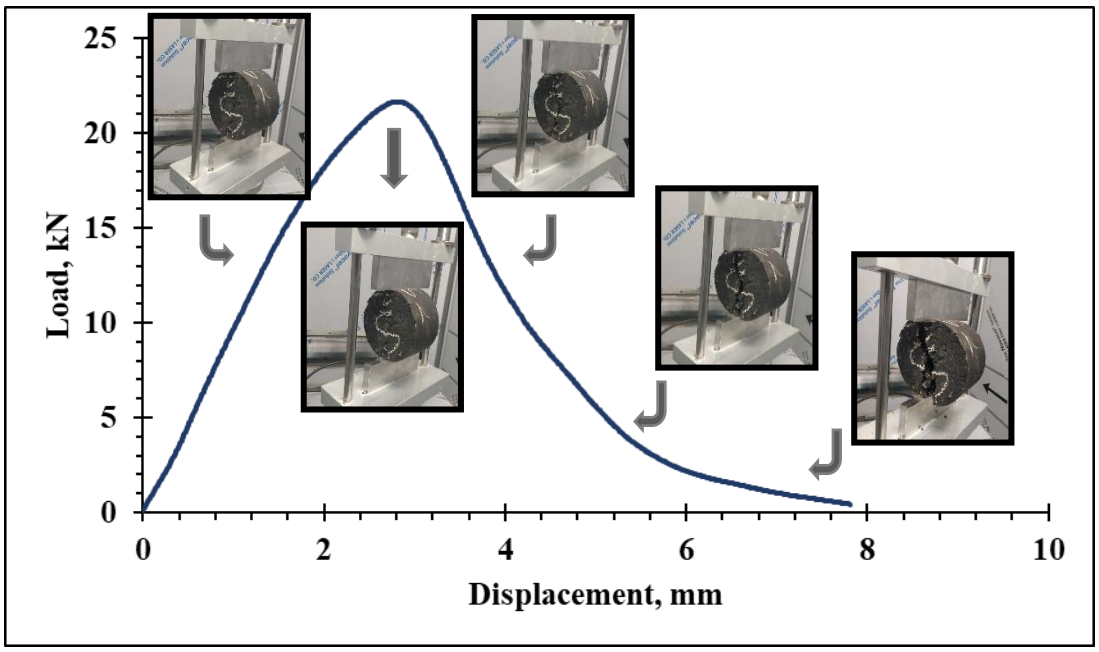

(b)

Figure 3.35. Ideal CT test (a) Setup in DTS-30, and (b) Schematic representation of the load-displacement curve

3.4.4.4 Moisture Resistance

The ingression of water into the pavement layers and the presence of significant moisture content generally reduce the bond between asphalt binder and mineral aggregate. This leads to a loss in the strength of the asphalt mix. The applicability of a single test for the evaluation of moisture resistance is impractical to a wide range of pavement materials and testing conditions. Thus, different tests (as follows) were performed to estimate the moisture sensitivity of asphalt mixtures

3.4.4.4.1 Boiling Water Test

The integrity of the adhesive bond between binder and mineral aggregate under wet conditions was assessed using a boiling water test (BWT). This test was developed by Kennedy et al. [508] in the year 1984 and later ASTM D3625 [509] proposed the standard guidelines. In order to evaluate the level of stripping, a visual rating protocol

was adopted by using the ratio of uncoated aggregates area to the area of coated loose aggregates. The visual rating was established by a team of 3 people using a lighted magnifying glass.

The experiment was performed on the loose mixes as per ASTM D3625 [509]. 200 grams of aggregates passing 20 mm and retained on a 12.5 mm sieve were taken and mixed with 5% asphalt binder (by weight of aggregates). The mixture was immersed in a beaker filled with 500 ml of water (Figure 3.36a) and was subjected to continuous heating under a controlled temperature range (85˚C to the boiling point of water) for 10 min. The mixture was allowed to cool (Figure 3.36b) and spread on a white paper towel. Visual inspection was done after drying the aggregates. Mixture which fails to meet the coating requirement of >85% is expected to have higher chances of stripping [510]. This was used as the pass/fail criterion in this study.

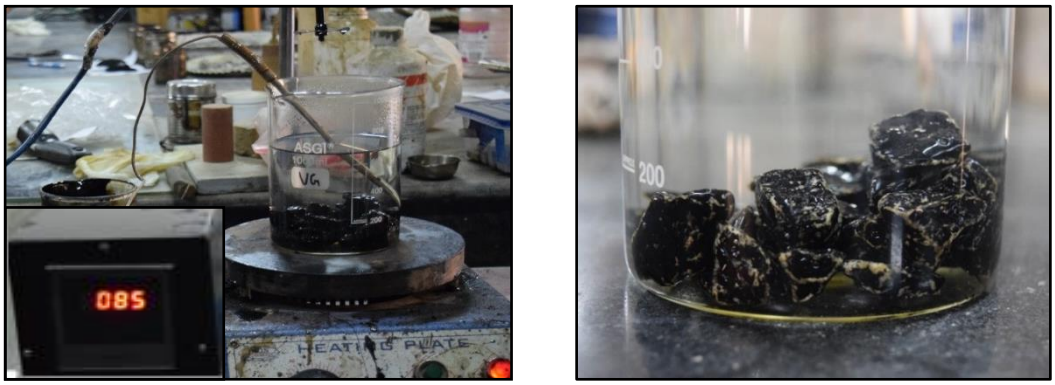

(a) (b)

Figure 3.36. Boiling water test (a) Boiling of the loose asphalt mixture at 85°C, and (b) Representation of stripping of asphalt binder from the aggregates after BWT

3.4.4.4.2 Retained Marshall Stability (RMS)

RMS was conducted to quantify the moisture sensitivity of asphalt mixtures. In this test method, Marshall stability was determined for dry and wet conditioned samples.

Marshall stability is defined as the maximum load carried by the compacted specimen. ASTM D6927 [511] was followed to determine the Marshall stability of HMA and WMA mixtures. Cylindrical specimens of 101.5 mm diameter and 63.5 mm height were prepared at predefined OBC and subjected to 75 blows on each side. The Marshall samples were placed in a temperature-controlled water bath at 60˚C for 30-40 minutes. Thereafter, the specimens were placed in the Marshall stability machine (Figure 3.37a), where it was subjected to a constantly (50.8 mm/minute) increasing load. The maximum load, along with the vertical deformation, was noted. This value of Marshall stability is defined as unconditioned Marshall stability. Additional replicates of Marshall compacted specimens were conditioned in the water bath (Figure 3.37b) at a temperature of 60˚C for 24 hours prior to testing. This is denoted as the conditioned Marshall stability value. RMS (equation 3.5) is defined as the ratio of Marshall stability of conditioned and unconditioned specimens.

$$RMS = \frac{Marshall\ stability_{\ conditioned}}{Marshall\ stability_{\ unconditioned}} \times 100 \qquad (3.5)$$

(a)

(b)

Figure 3.37. Retained Marshall stability test (a) Marshall testing apparatus, and (b) Compacted specimens in water bath

3.4.4.4.3 Modified Lottman Test

The modified Lottman test has been most often used to evaluate the effect of moisture on compacted asphalt mixtures. In this test method, indirect tensile strength *(ITS)* of compacted asphalt mixtures, prepared at OBC with 7% air voids, is determined in dry and wet conditioned states according to AASTHO T283 [344]. The unconditioned compacted specimens were immerged in the water bath at 25 °C for 2 hours followed by the testing under the loading condition parallel to the sample's vertical diametric plane (Figure 3.38a). The adopted loading configuration creates uniform stress on the specimen under testing, which is tensile in nature, acting perpendicular to the direction of load and parallel to the vertical diametric plane. The load is applied at a 50.8 mm/minute rate using the *ITS* test apparatus (Figure 3.38b), and the maximum load *(P_{max})* at which the compacted specimen fails was noted. In the case of conditioned state, the samples were immersed in the water bath maintained at 60 °C for 24 hours. After 24 hours, the specimens were removed and kept in a water bath for 2 hours at 25 °C before testing. The ratio of *ITS* value (equation 3.6) for conditioned and unconditioned state samples is defined as Tensile strength ratio *(TSR)* (equation 3.7), which should be typically > 80% for better moisture resistance.

$$ITS = \frac{2000P_{max}}{\pi td} \tag{3.6}$$

$$TSR = \frac{ITS\ conditioned}{ITS\ unconditioned} \times 100 \tag{3.7}$$

Where *ITS* is the indirect tensile strength in (kPa), P_{max} is the peak load (N), *t* is the thickness of the specimen (mm), and *d* is the diameter of the specimen (mm).

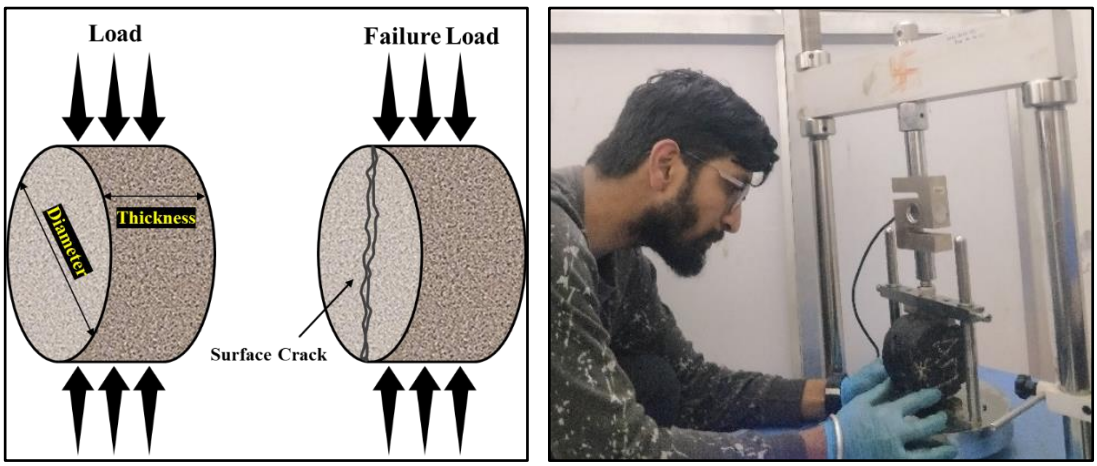

(a) (b)

Figure 3.38. Modified Lottman test (a) *ITS* test loading representation, and (b) *ITS* test apparatus

3.5 Summary

This chapter presented the details of the materials and experimental framework used in the present study. The experimental work was carried out in different phases, starting from the initial testing plan, which involves the evaluation of production temperatures of WMA mixtures, followed by their characterization based on binders and mixtures testing. Notably, the performance testing was executed on the asphalt binders and mixtures prepared with the optimum dosage of WMA additives. Different binder types, aggregate sources, test temperatures, stress/strain values, and frequencies were chosen to broadly investigate the performance of WMA binders and mixtures relative to conventional HMA. Emphasis was given to the ageing mechanism of asphalt binder and mixtures, irrespective of the binder type and aggregate source. Frequency sweep and FTIR were conducted on UA, STA and LTA to adjudge the impact of WMA additives on the ageing characteristics of the asphalt binders.

Some primary material characterization results were also described in this chapter. A brief summary of the results is as follows:

SEM and FTIR confirmed that the adopted blending technique is appropriate for obtaining the uniform/homogeneous blend with pure physical interaction between WMA additives and asphalt binders. However, the variations were observed in the FTIR Spectra of VG30 and PMB40. Sasobit Redux, Rediset and Cecabase did not influence the physical characteristics (penetration and softening point, and viscosity) and high-temperature PG. On the other hand, incorporating Sasobit increased the softening point, viscosity, and true fail temperature and reduced the penetration value, irrespective of the base asphalt binder.